Geological and Petrophysical Evaluation of Sandstone Cores in the Great Burgan Field in Kuwait*

Osama Al-Jallad[1], Moustafa Dernaika[1], Safouh Koronfol[1], Mona Rashaid[2], and Laila Hayat[2]

Search and Discovery Article #20403 (2017)**
Posted September 18, 2017

*Adapted from oral presentation given at 2017 AAPG Middle East Region Geoscience Technology Workshop, Siliciclastic Reservoirs of the Middle East, Amman, Jordan, May 15-16, 2017

[1]Ingrain Inc. (aljallad@ingrainrocks.com)
[2]Kuwait Oil Company (KO

Abstract

In Kuwait, the Southeast Great Burgan Field possesses the world's largest sandstone oil reservoirs both in terms of reserves and production (Kirby et al., 1998; Sorkhabi, 2012). It comprises three giant sectors: Burgan, Ahmadi, and Magwa which are characterized by their domal structure (Carman, 1996; Kaufman et al., 2002). The 28-36° API mature oil is produced predominately from two Mid-Cretaceous (Late Albian to Early Cenomanian) sandstone reservoirs, the Wara and Burgan formations (Kaufman et al., 2002; Strohmenger et al., 2006). Both formations were deposited in a fluvial deltaic environment on the continental shelf margin of the ancient Tethys Ocean (Kirby et al., 1998; Sorkhabi, 2012).

The Burgan sandstone (BF) succession consists of two units, the third and fourth sands. The third sand succession is divided into three members, the lower, middle and upper (Kaufman et al., 2002; Datta et al., 2012; Sorkhabi, 2012). On the other hand, Wara sandstone (WF) succession is divided into first and second units (Sorkhabi, 2012). Both formations are separated by a carbonate succession of the Mauddud Formation which was deposited in a shallow marine environment (Kirby et al. 1998; Strohmenger et al., 2006). In this research, whole cores extracted from the Upper Burgan (UBF) and WF in the Burgan and Ahmadi fields were evaluated using an integrative workflow combining Digital Core Analysis (DRA) methods with conventional techniques. This integrative workflow provided improved understanding of the geological and petrophysical properties of these oil prolific reservoirs.

References Cited

Carman, G.J., 1996, Structural elements of onshore Kuwait: GeoArabia, v. 1/2, p. 239-266.

Kaufman, R.L., H. Dashti, C.S. Kabir, J.M. Pederson, M.S. Moon, R. Quttainah, and H. Al-Wael, 2002, Characterizing the Greater Burgan Field: Use of Geochemistry and Oil Fingerprinting: Society of Petroleum Engineers. doi:10.2118/78129-PA.

Kirby, R.H., B.S. Carr, J. Al-Humoud, A.I. Safar, D. Al-Matar, and W. Naser, 1998, Characterization of a vertically compartmentalized reservoir in a supergiant field, Burgan Formation, Greater Burgan Field, Kuwait, Part 1: Stratigraphy and Water Encroachment: Society of Petroleum Engineers. doi:10.2118/49214-MS.

Sorkhabi, R., 2012, The Great Burgan Field, Kuwait: GEOExPRO Magazine, v. 9/1, p. 42-63.

Strohmenger, C.J., P.E. Patterson, G. Al-Sahlan, J.C. Mitchell, H.R. Feldman, T.M. Demko, R.W. Wellner, P.J. Lehmann, G.G. McCrimmon, R.W. Broomhall, and N. Al-Ajmi, 2006, Sequence stratigraphy and reservoir architecture of the Burgan and Mauddud Formations (Lower Cretaceous), Kuwait, *in* P.M. Harris, and L.J. Weber, eds., Giant Hydrocarbon Reservoirs of the World: From Rocks to Reservoir Characterization and Modeling: AAPG Memoir 88, p. 213-245.

AAPG
Advancing the World of Petroleum Geosciences.

GEOLOGICAL AND PETROPHYSICAL EVALUATION OF SANDSTONE CORES IN THE GREAT BURGAN FIELD IN KUWAIT

Osama Al-Jallad[1], Moustafa Dernaika[1], Safouh Koronfol[1], Mona Rashaid[2]and Laila Hayat[2]

[1] Ingrain Inc., [2] Kuwait Oil Company

INGRAIN

Kuwait Oil Company
A Subsidiary of Kuwait Petroleum Corporation

AAPG
Advancing the World of Petroleum Geosciences.

Presentation Outline

- Introduction:
  - Geological Settings.
  - Study Objectives.
- Methodology.
- Results and Data interpretation:
  - DE and Micro Scanning.
  - Petrography.
  - DE Scanning.
  - Mercury Injection.
  - Poroperm.
  - XRD Analysis.
  - XCT Imaging
  - Numerical Computation.

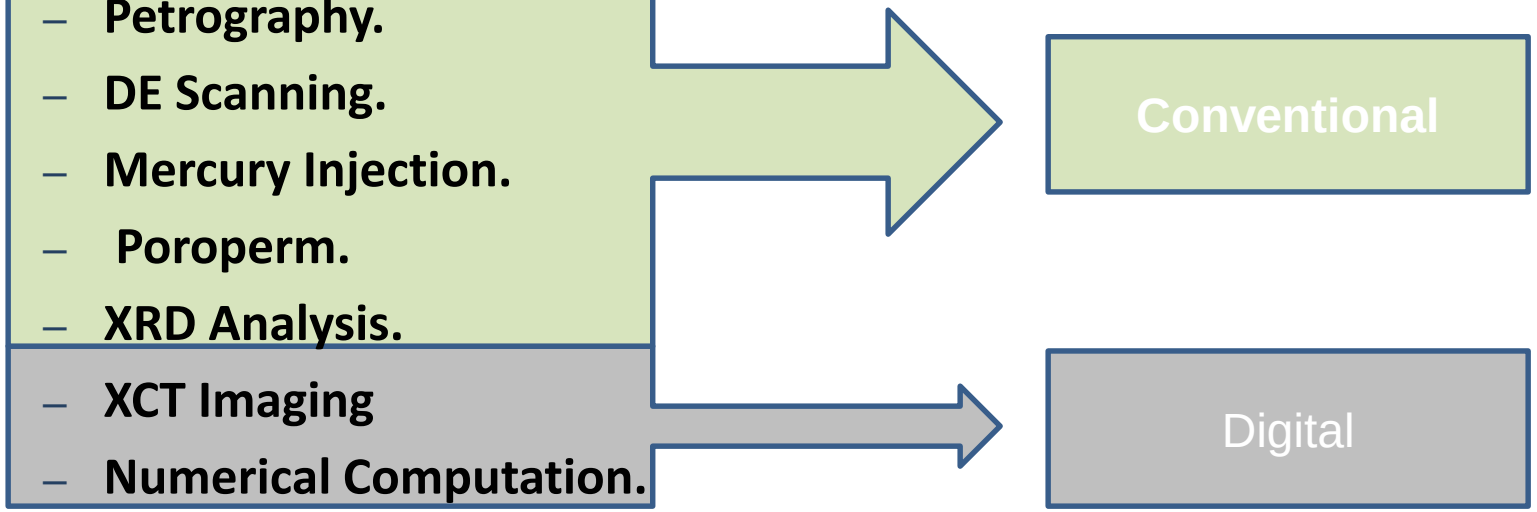

- Summary and Conclusion.

AAPG
Advancing the World of Petroleum Geosciences.

Introduction: Geological Settings

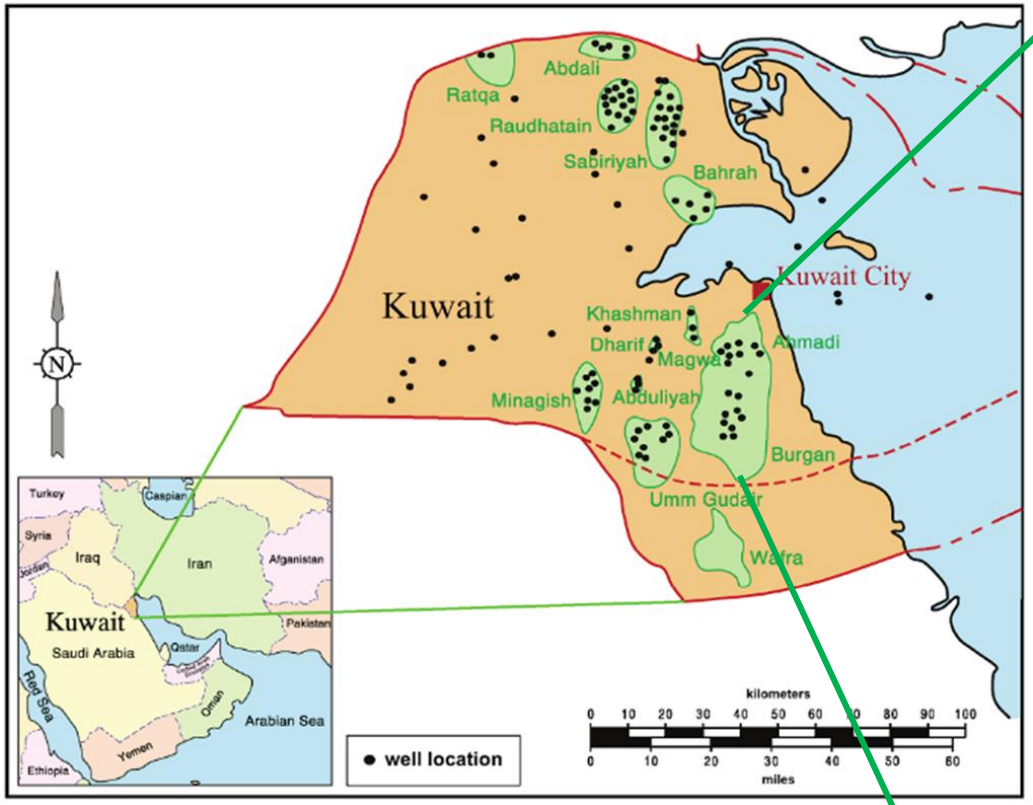

Modified after Carman,. 1996 and Strohmenger et al., 2006

The South East Great Burgan Field possesses the world's largest sandstone oil reservoirs both in terms of reserves and production (Kirby et al. 1998)

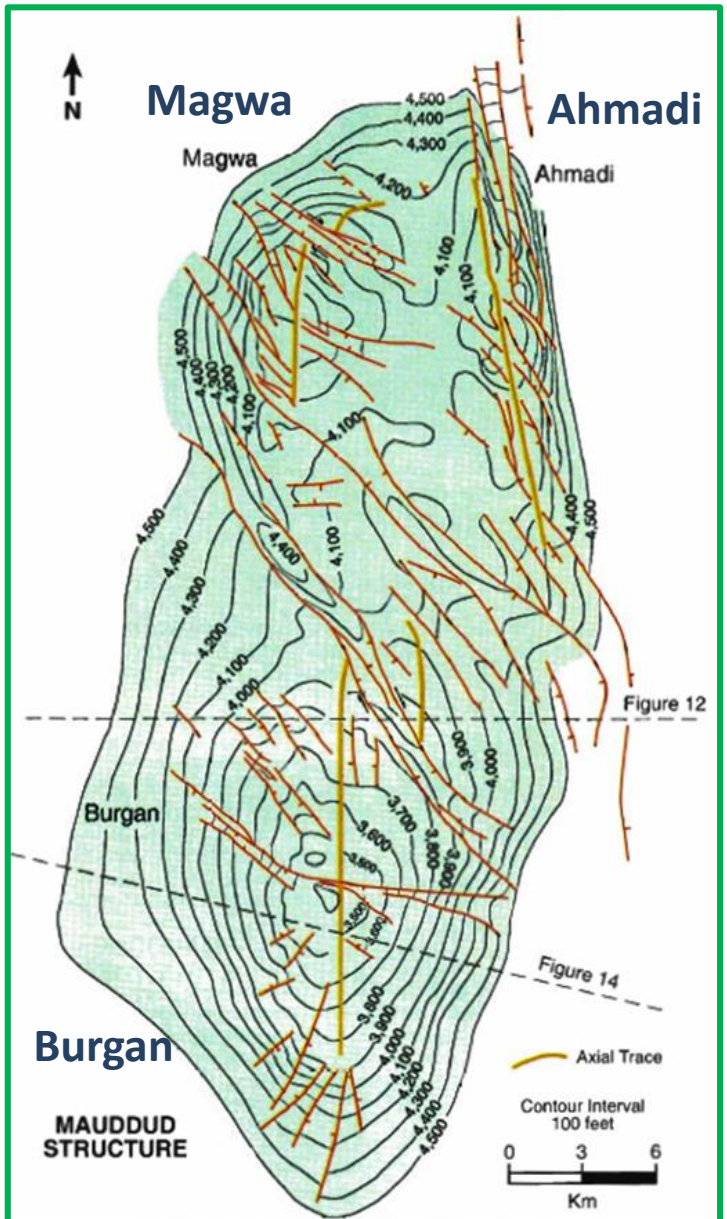

Introduction: Geological Settings

- The 28-36° API mature oil is produced predominately from two Mid-Cretaceous (late Albian to early Cenomanian) sandstone reservoirs; Wara and Burgan formations (Kaufman et al., 2002).
- Both formations were deposited in a fluvial deltaic environment on the continental shelf margin of the ancient Tethys Ocean (Kirby et al. 1998).
- Both formations are separated by carbonate succession of Mauddud Formation which deposited in a shallow marine environment

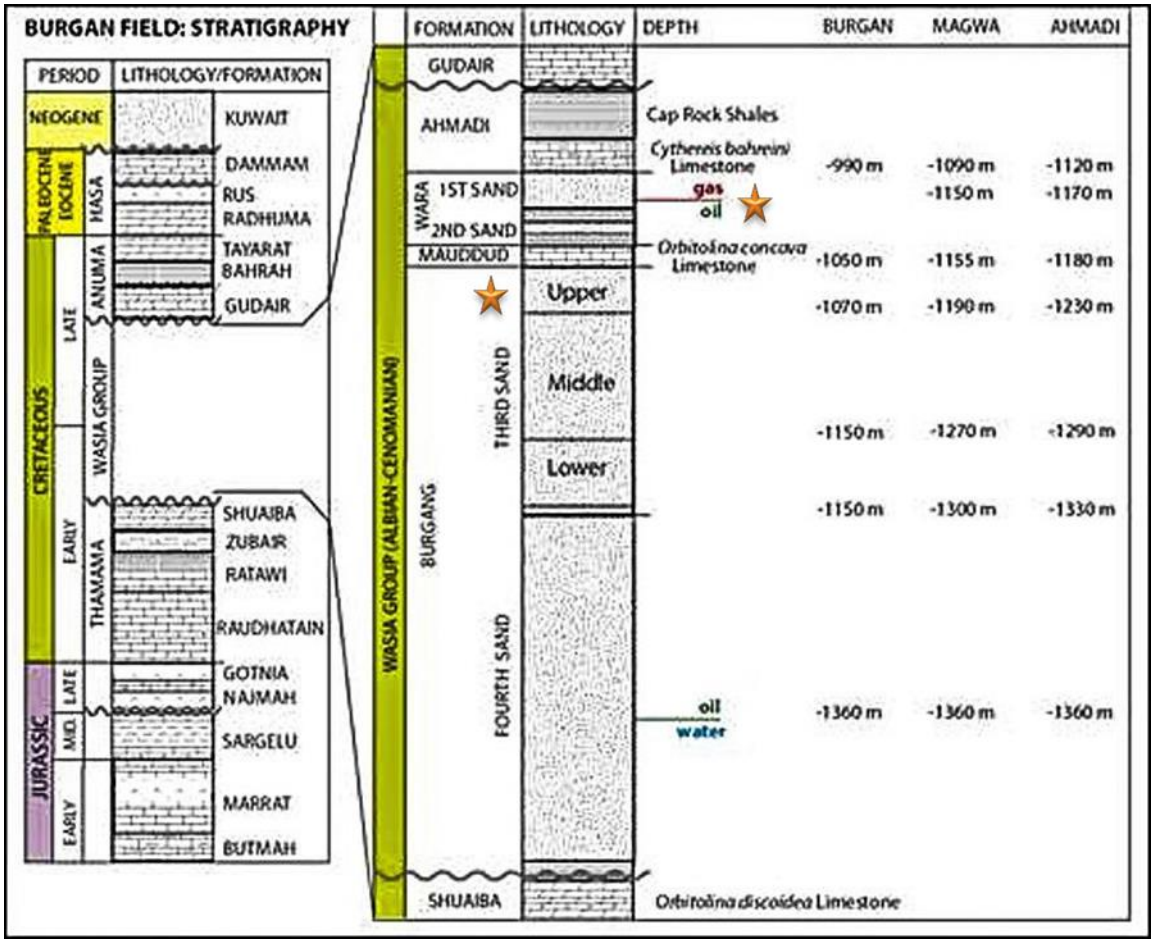

Modified after Sorkhabi, 2012

Introduction: Study Objectives

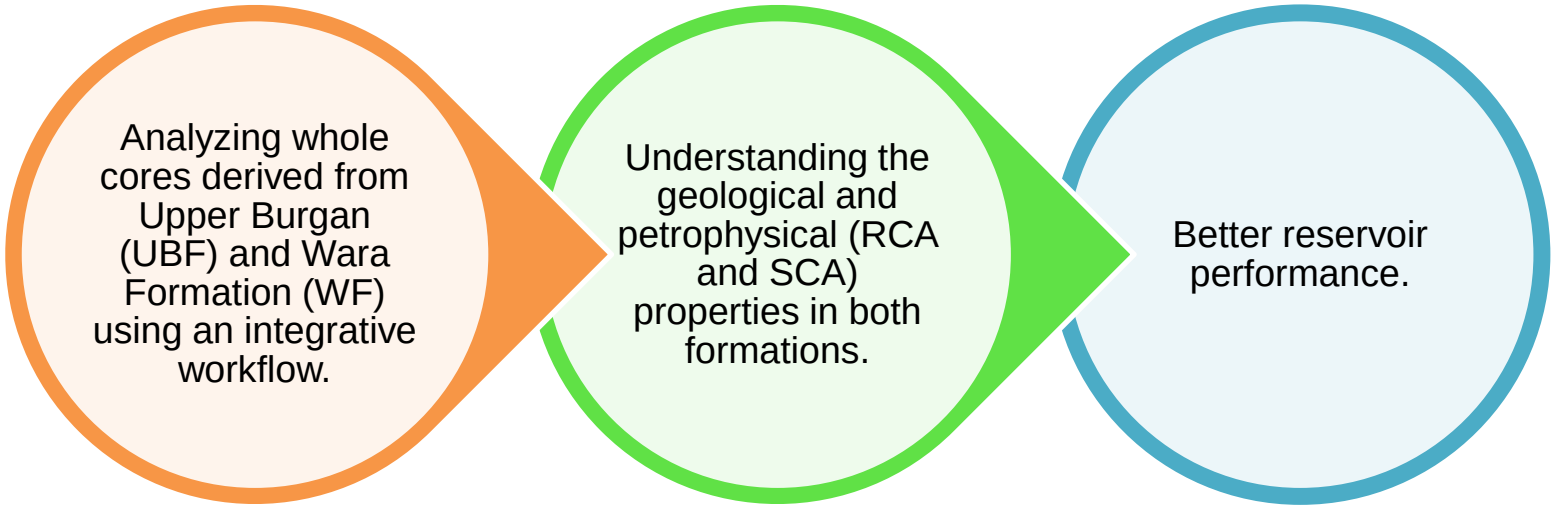

Methodology and Workflow

Digital Rock Analysis (DRA)

Conventional Rock Analysis

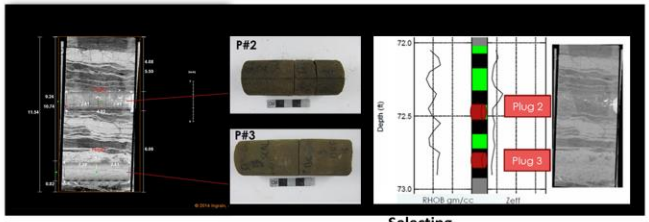

Dual Energy CT Scanning

Selecting Plugging Location and Sample Extractions

Plug Dual Energy Scanning

40 µm/voxel XCT Imaging and Wafers Selections and Cutting

Conventional Analysis

High Resolution Imaging

Integration between convention al data and CT Images

Core Plugs Segmentation

Properties Upscaling

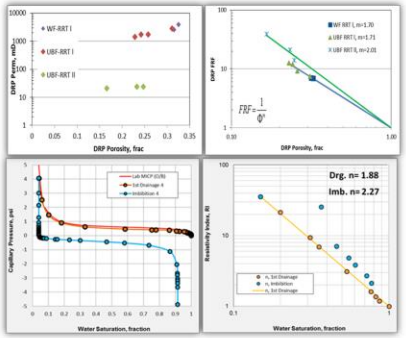

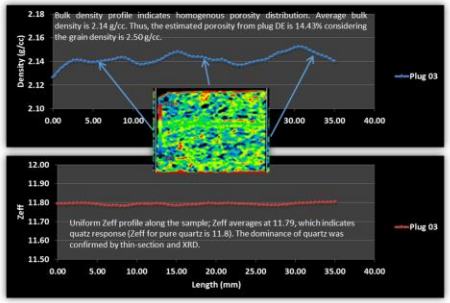

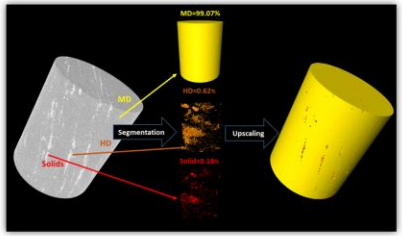

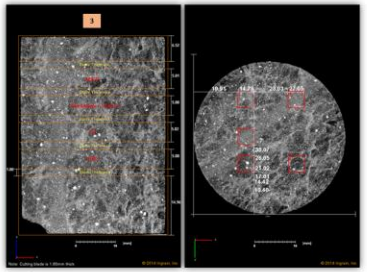

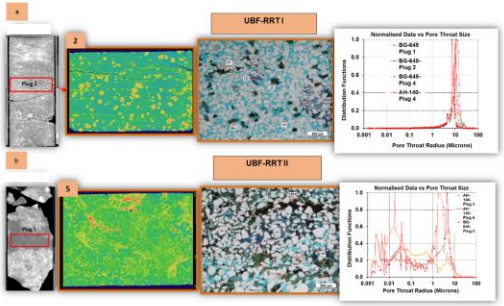

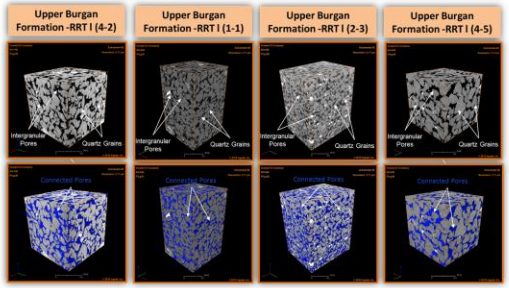

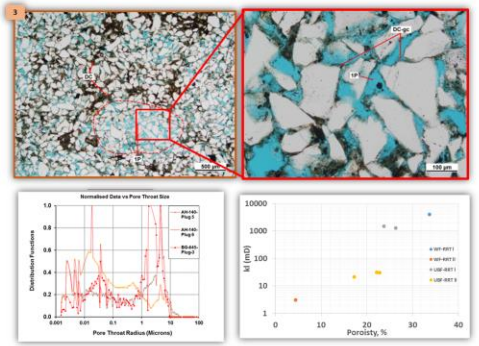

Results and Data interpretation: Whole Core DE Scanning

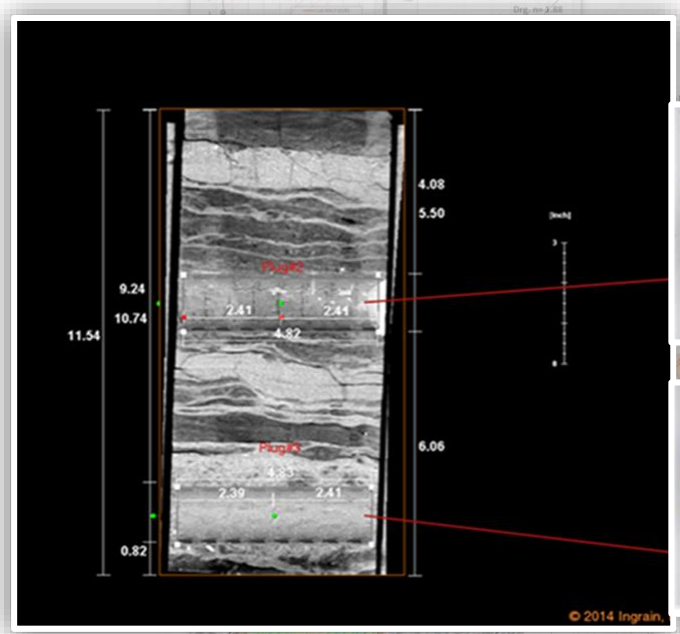

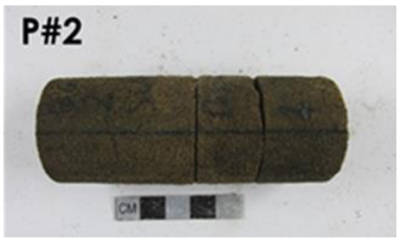

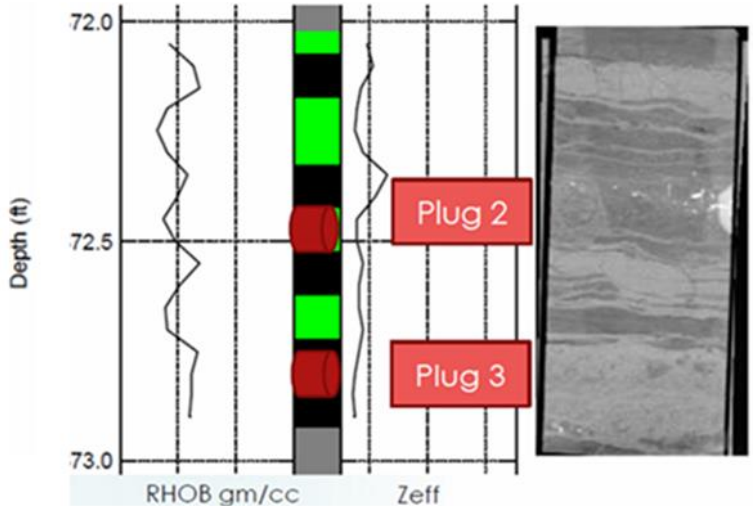

Results and Data interpretation: Core Characterization

AAPG
Advancing the World of Petroleum Geosciences.

xx8 -xx99 ft
C1-T06

xx20- xx21 ft
C3-T14

Field	WC-Tray	Depth Interval (ft)	Formation
Ahmadi	C1-T06	xx98 -xx99	WU
	C1-T09	xx08-xx09	WM1
	C2-T11	xx64-xx65	WM1
	C3-T06	xx88-xx89	WL1
	C3-T14	xx20-xx21	WL1
	C5-T15	xx21-xx22	BU2
	C6-T04	xx57-xx58	BU2
	C6-T11	xx88-xx89	BU2
	C7-T03	xx99-xx00	BU3
Burgan	C3-T10	xx38-xx39	BU2
	C4-T02	xx67-xx68	BU3
	C4-T04	xx72-xx73	BU3
	C4-T04	xx75-xx76	BU3
	C4-T07	xx87-xx88	BU3
	C4-T08	xx88-xx89	BU3

xx38 -xx39 ft
C3-T10

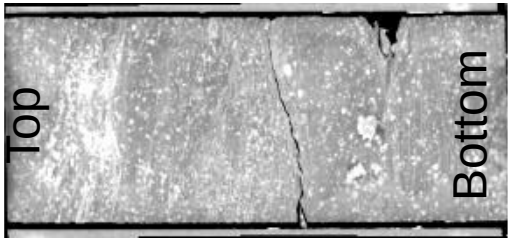

xx87- xx88 ft
C4-T07

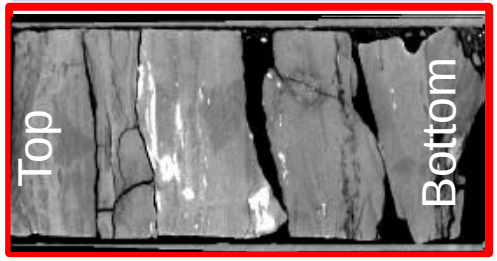

xx57- xx58 ft
C6-T04

xx99- xx00 ft
C7-T03

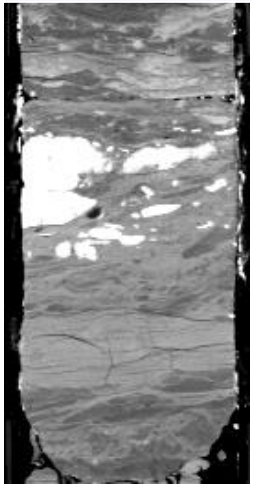

Results and Data interpretation: Core Characterization

AAPG
Advancing the World of Petroleum Geosciences.

Wara Formation Cores	Upper Burgan Fomration Cores

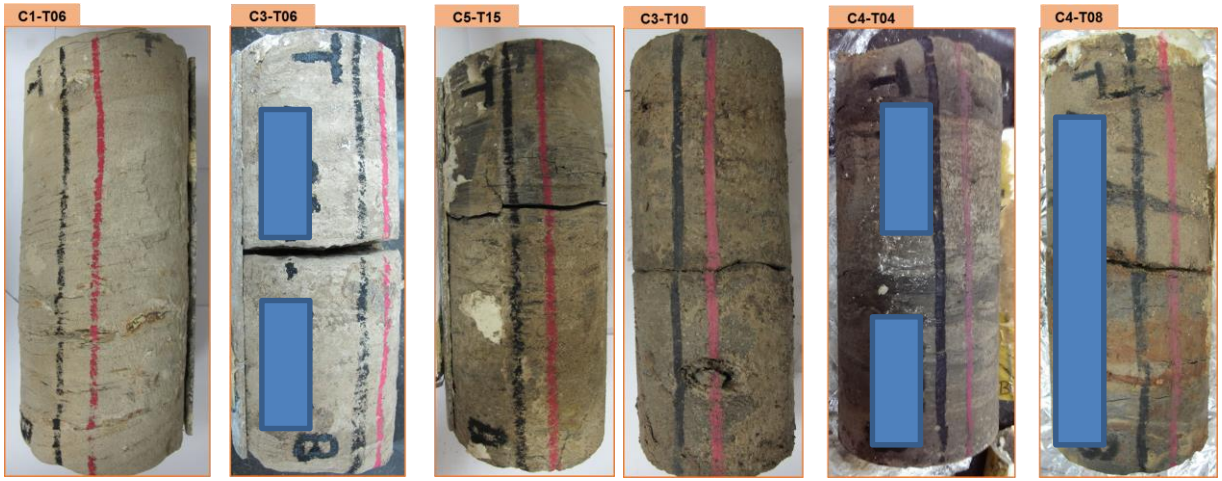

DE XCT Scanning (500 µm/voxel)

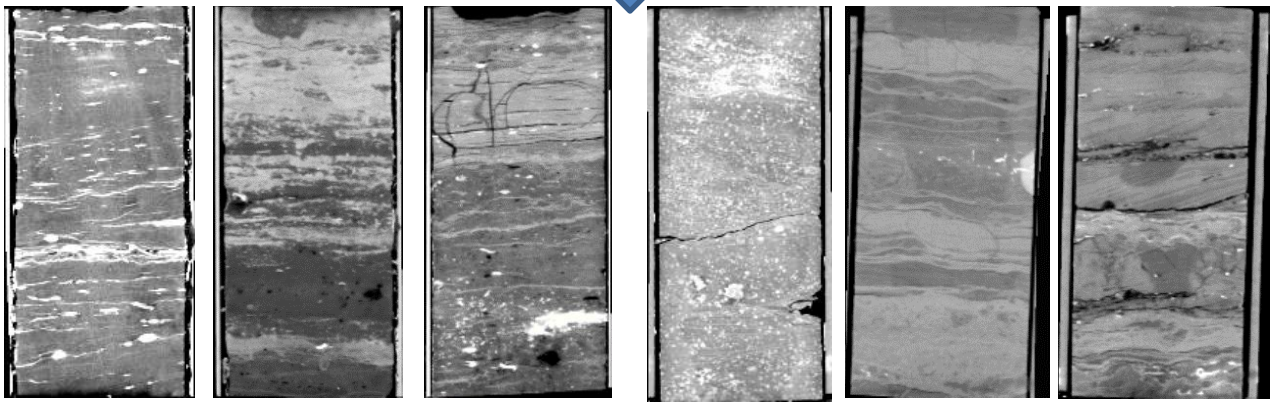

The cores are highly heterogeneous with alternating layers of massive and laminated sandstone. Also, scattered patches of high dense minerals and vuggy pores were observed as well.

Results and Data interpretation: Core Characterization

AAPG
Advancing the World of Petroleum Geosciences.

Wara Formation Cores	Upper Burgan Formation Cores

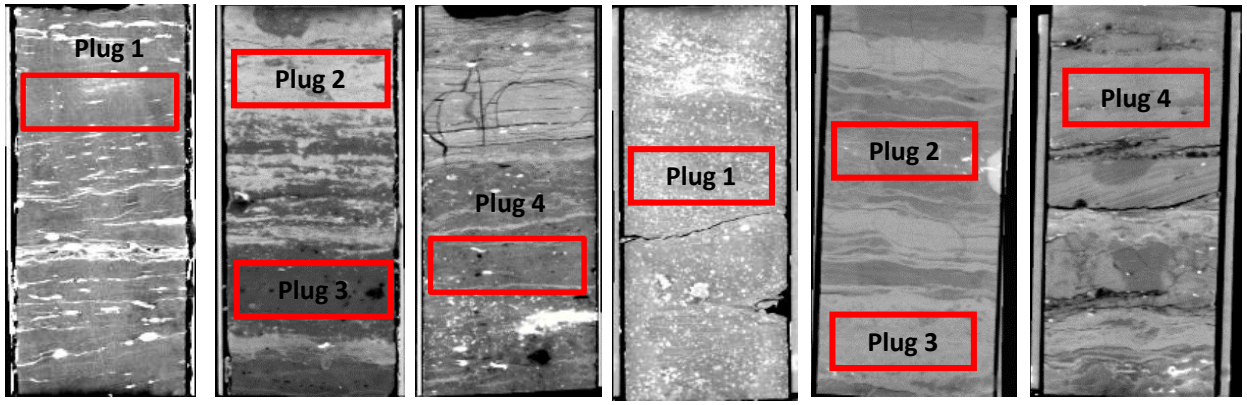

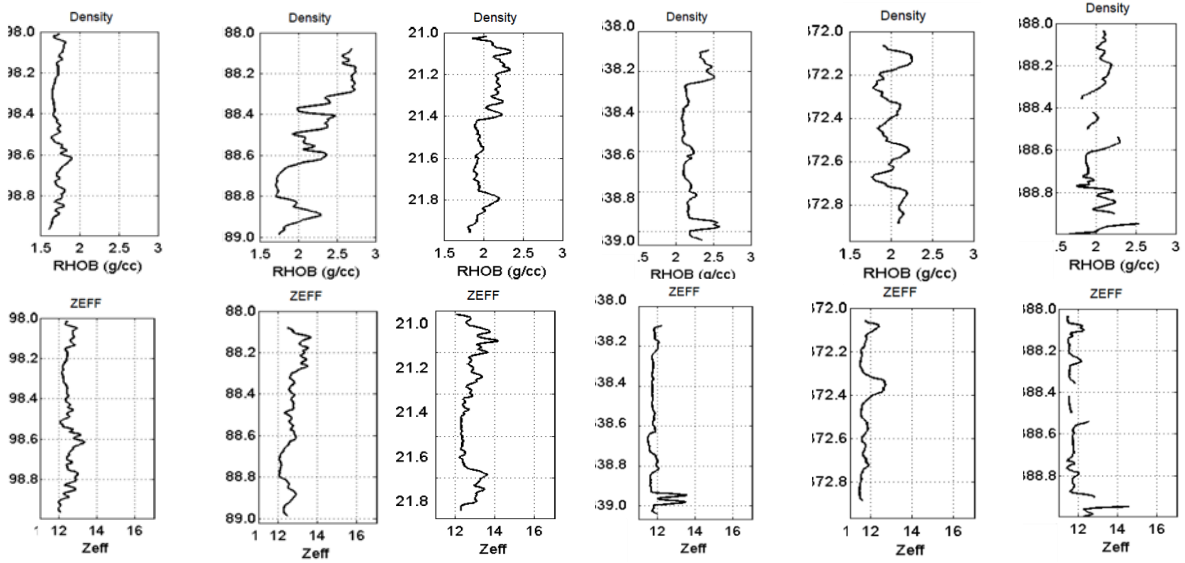

The generated Rhob logs reflect the variability of porosity distributions along the length of these cores.

The generated Zeff logs show average Zeff response equal to 11.8.

Results and Data interpretation: Plug Extraction and DE Scanning

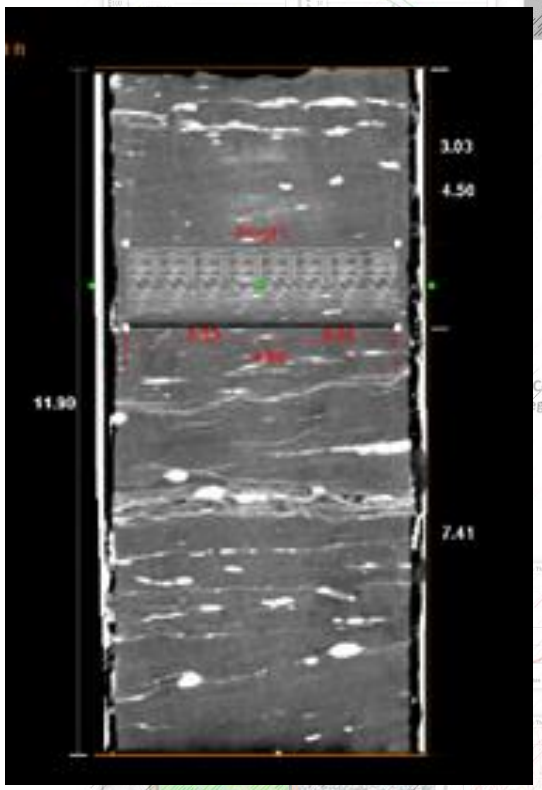

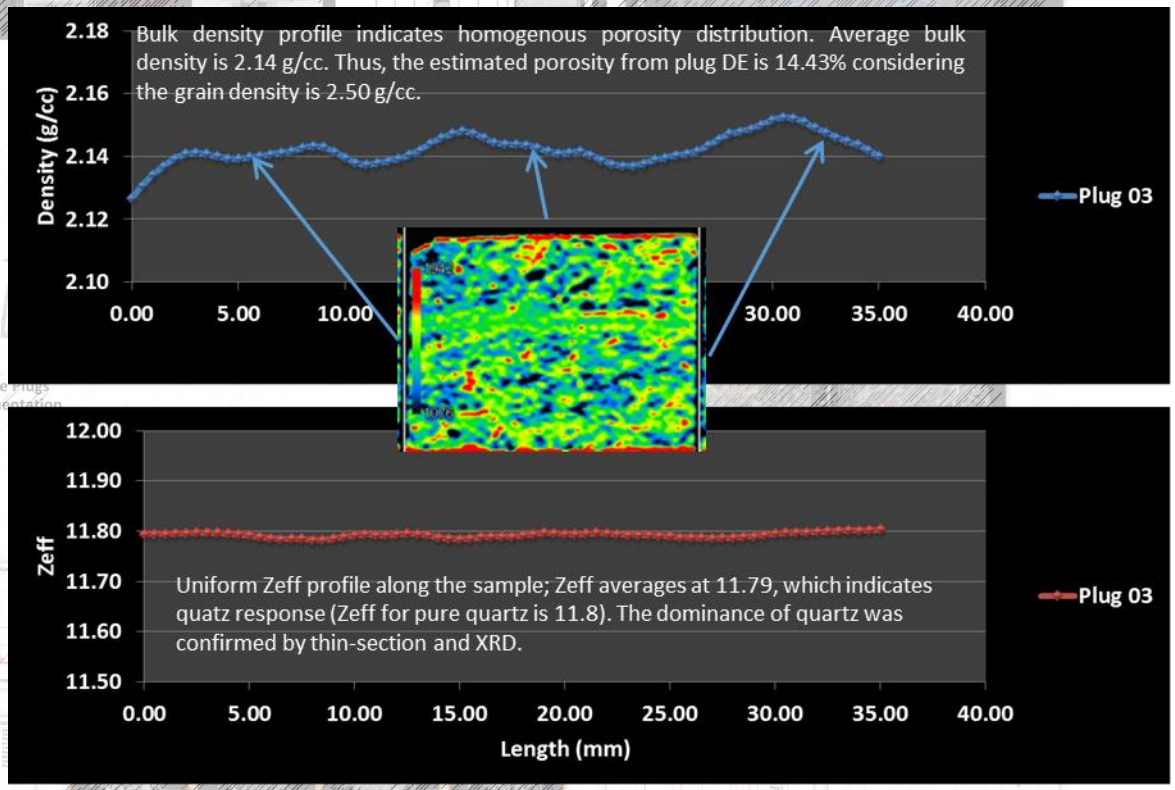

Results and Data interpretation: Core Plugging and DE Scanning

AAPG
Advancing the World of Petroleum Geosciences.

Wara Formation Cores

Upper Burgan Formation Cores

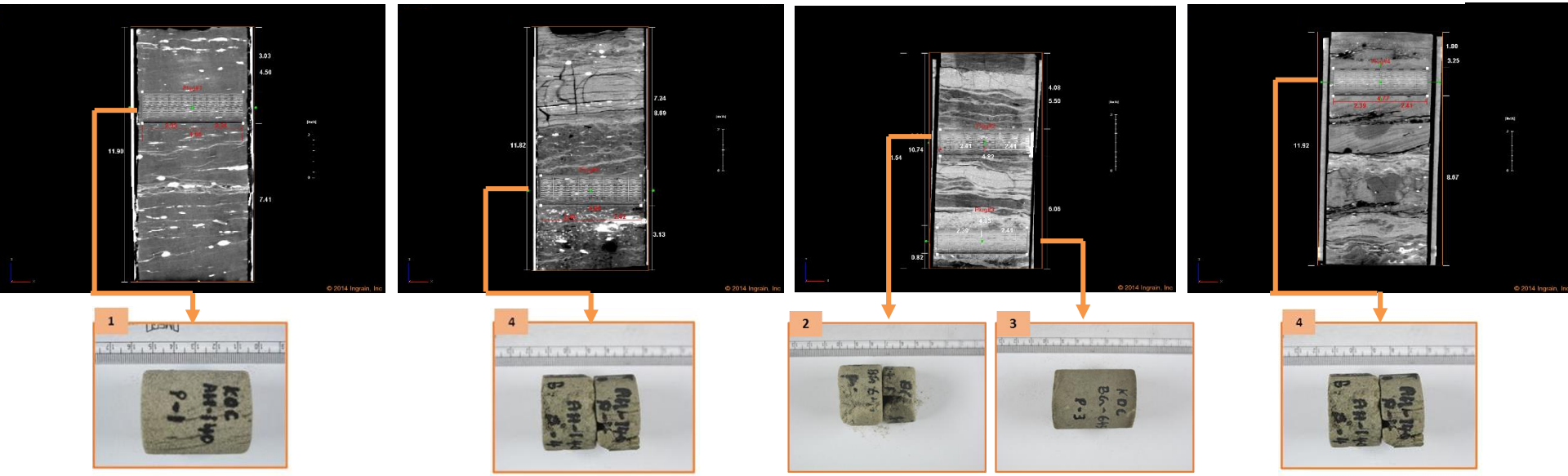

DE XCT Scanning (500 µm/voxel)

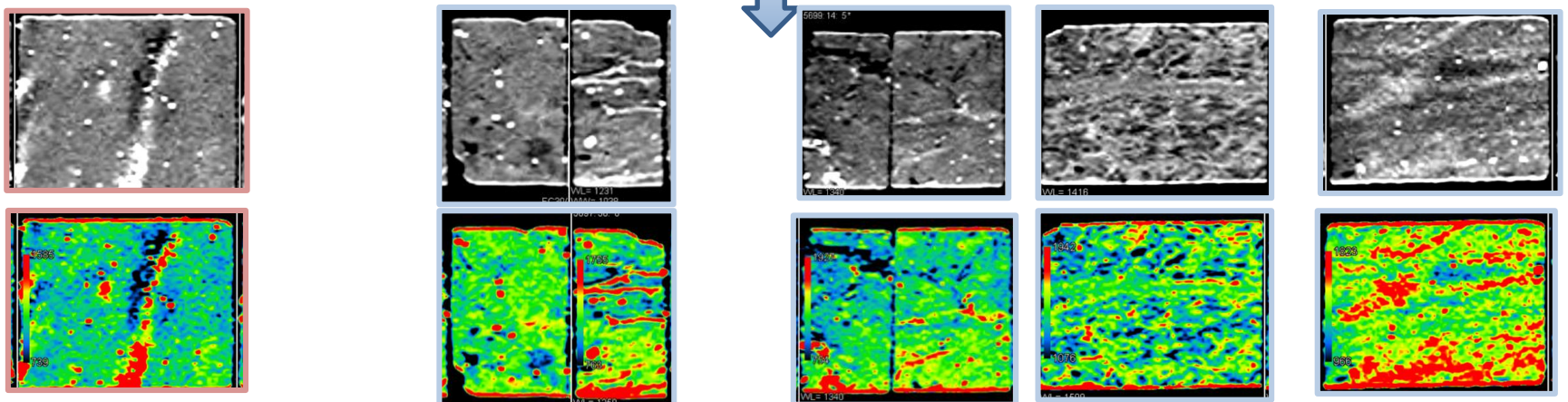

Results and Data interpretation: Core Plugging and DE Scanning

Plug DE XCT Scanning (500 µm/voxel)

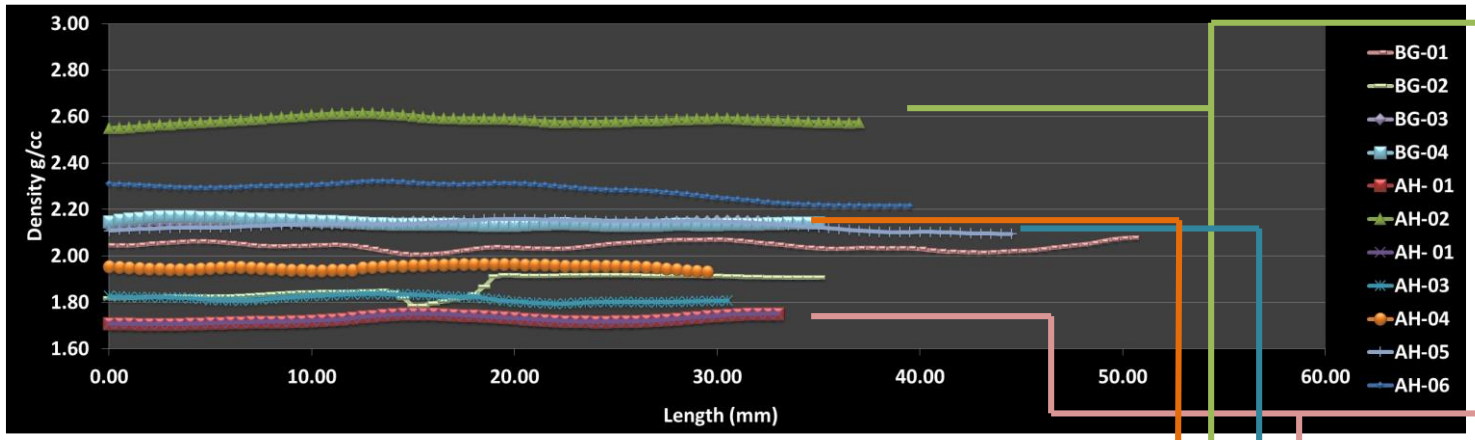

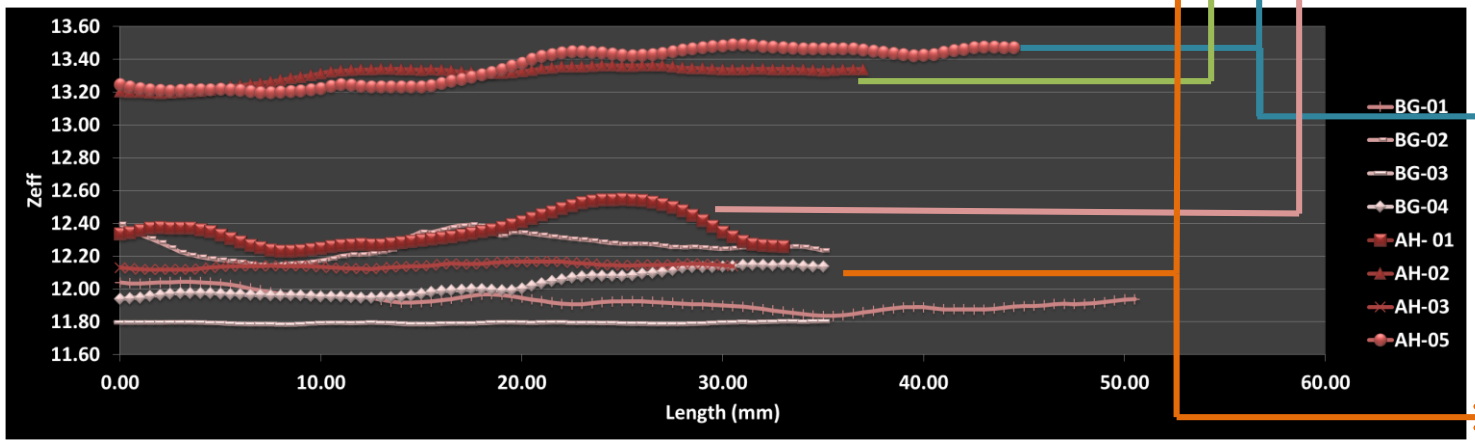

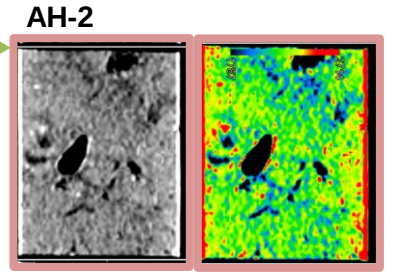

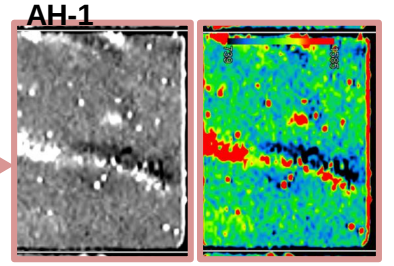

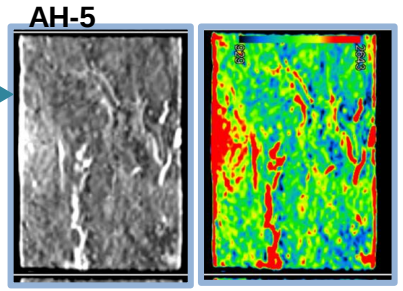

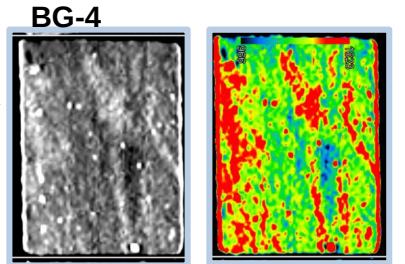

Results and Data interpretation: Plugs Characterization

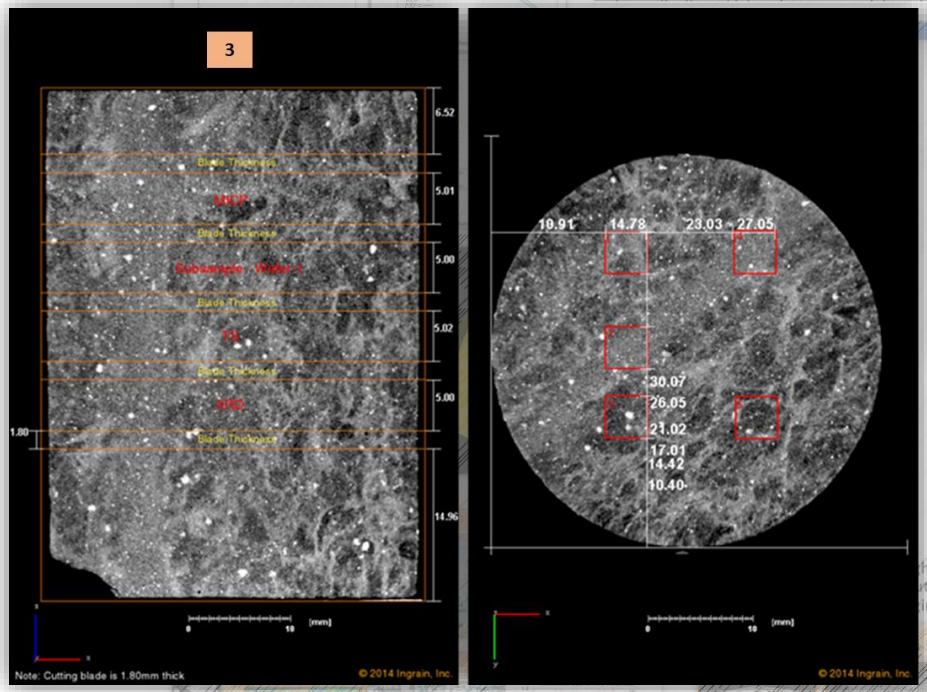

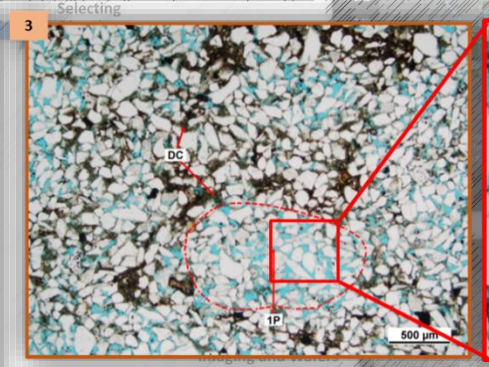

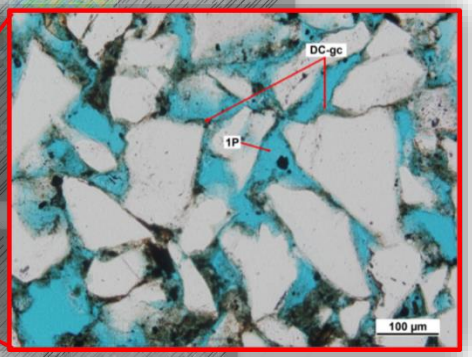

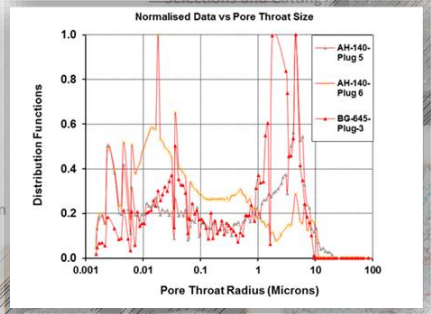

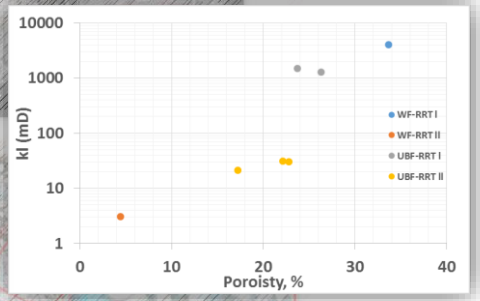

Results and Data interpretation: Micro CT Scanning (40 µm/voxel)

AAPG
Advancing the World of Petroleum Geosciences.

AH Field (Wara Formation)

AH&BG Field (Upper Burgan Formation)

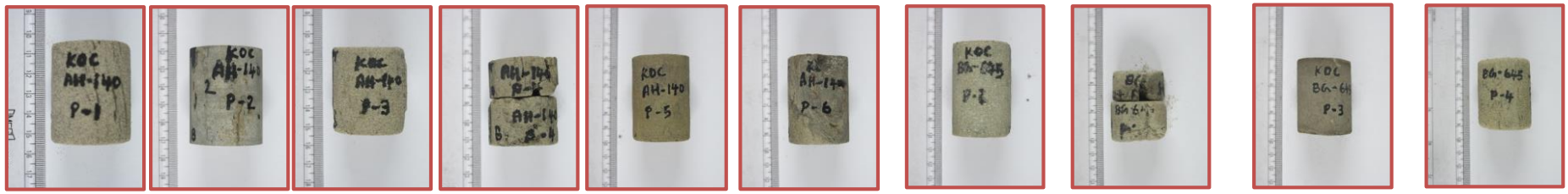

Micro XCT Scanning (40 µm/voxel)

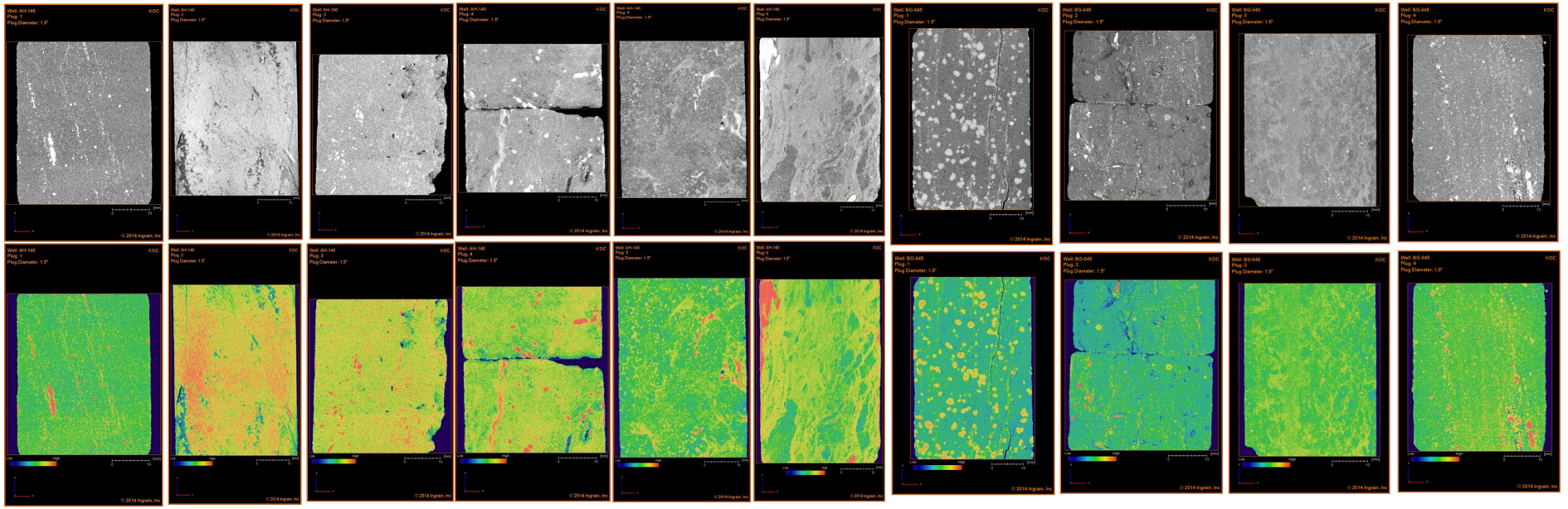

Plug 1	Plug 2	Plug 3	Plug 4	Plug 5	Plug 6	Plug 1	Plug 2	Plug 3	Plug 4

AAPG
Advancing the World of Petroleum Geosciences.

Results and Data interpretation: 40 µm/voxel Wafers Selections

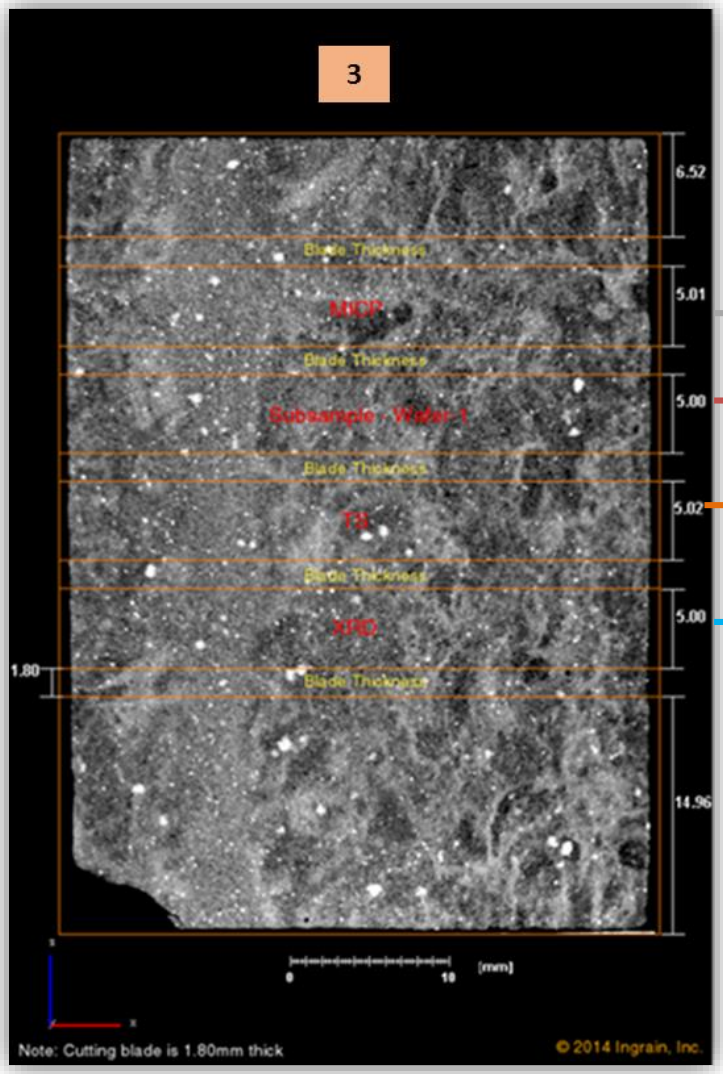

MICP

Subsamples

TS

XRD

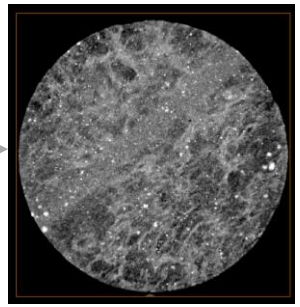

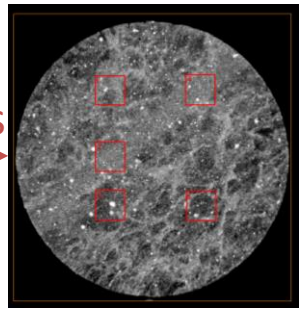

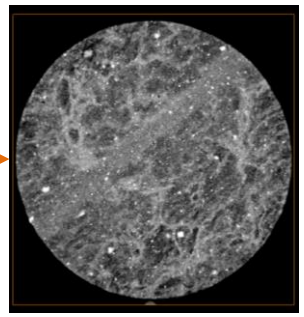

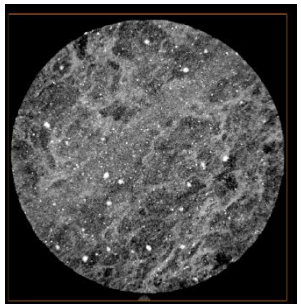

AAPG
Advancing the World of Petroleum Geosciences.

Results and Data interpretation: Petrographical Analysis

AH Field (Wara Formation)

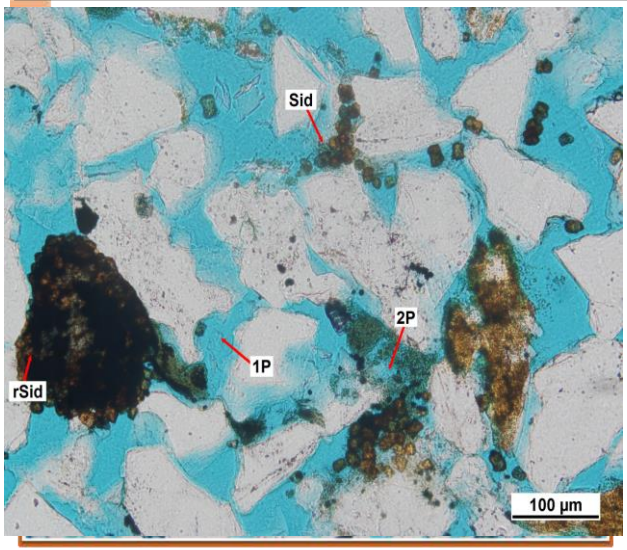

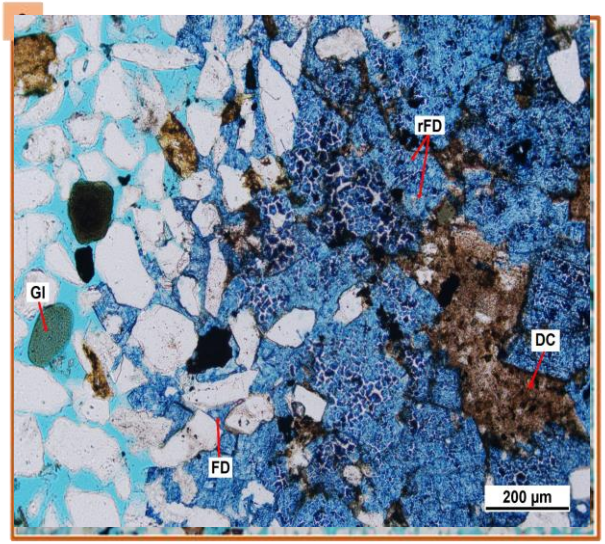

BG Field (Upper Burgan Formation)

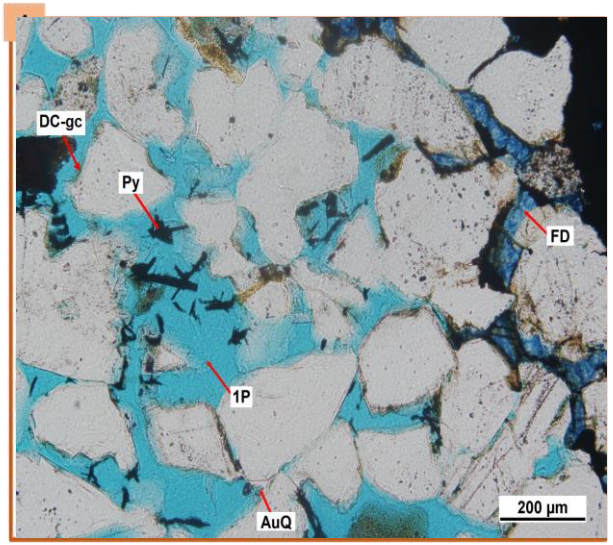

BG Field (Upper Burgan Formation)

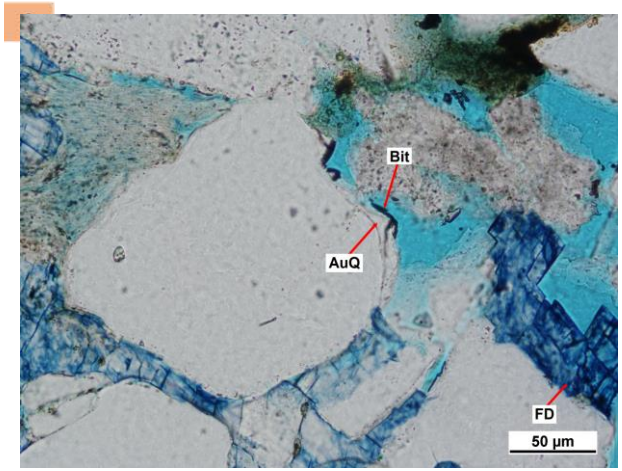

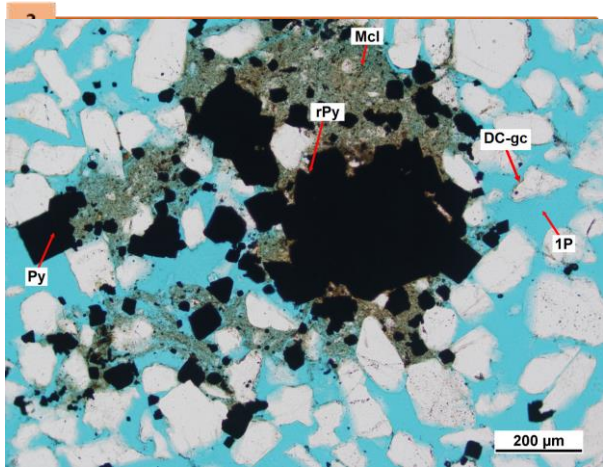

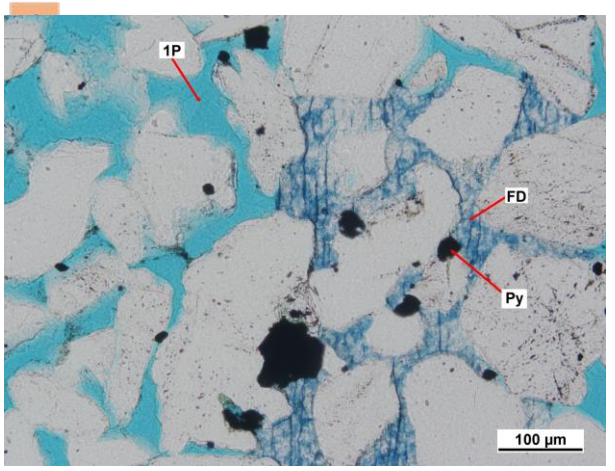

Results and Data interpretation: Petrographical analysis

AH Field (Wara Formation)

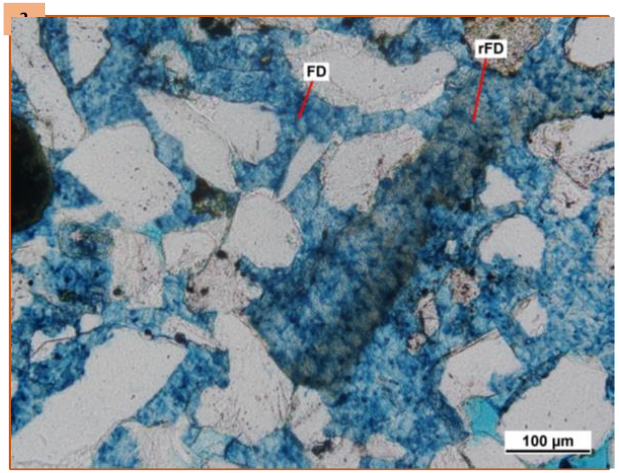

BG Field (Upper Burgan Formation)

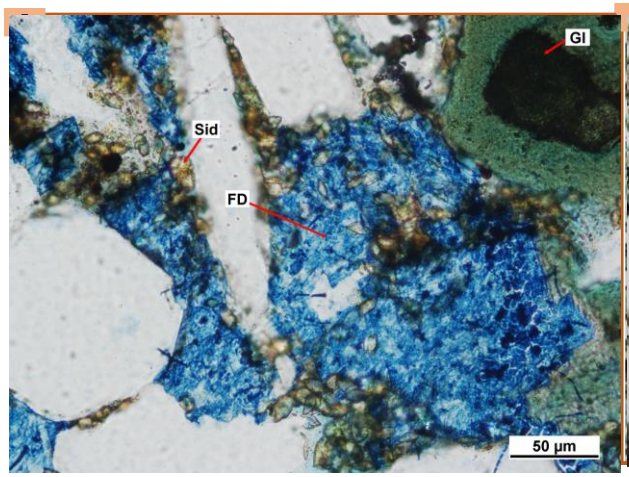

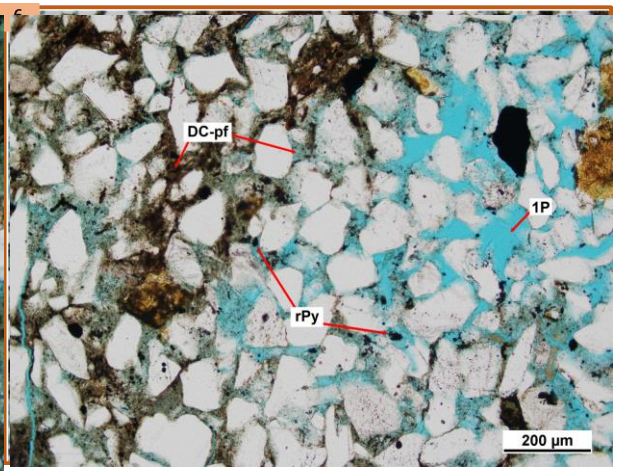

BG Field (Upper Burgan Formation)

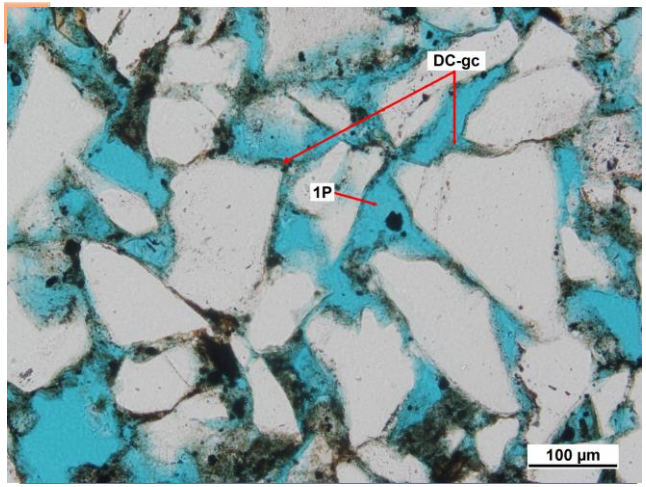

Results and Data interpretation: XRD Analysis

AH Field (Wara Formation)

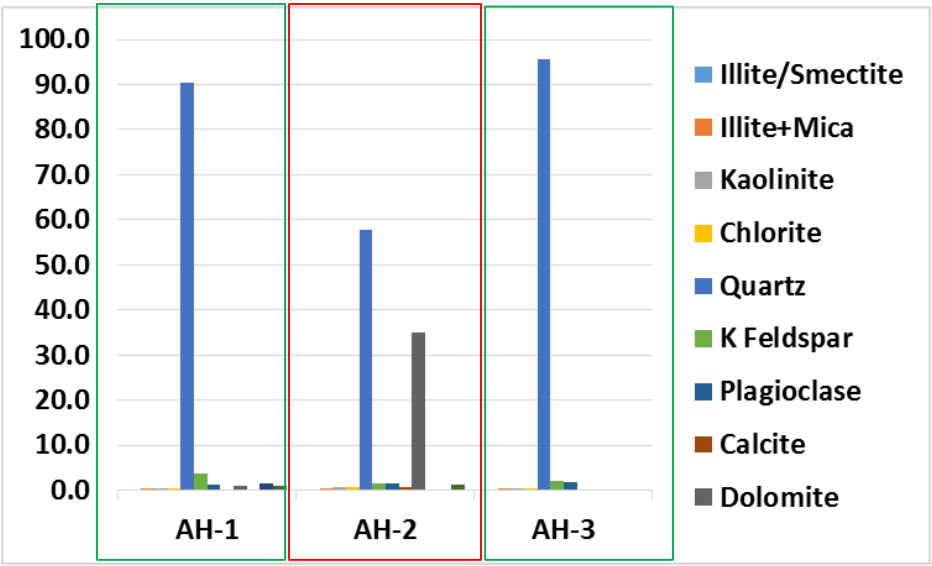

AH Field (Upper Burgan Formation)

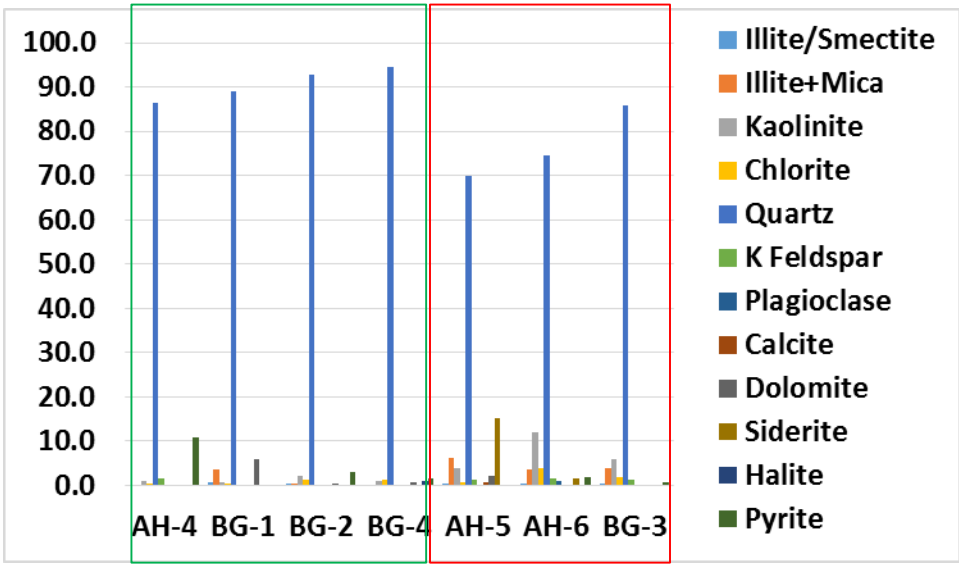

The majority of the Wara and Upper Burgan samples are composed mainly of Quartz with minor concentrations of pyrite.

Other few samples are made mainly quartz with considerable concertations of clay minerals such as kaolinite, illite, and chlorite as well as other authigenic minerals.

Results and Data interpretation: Poroperm and MICP

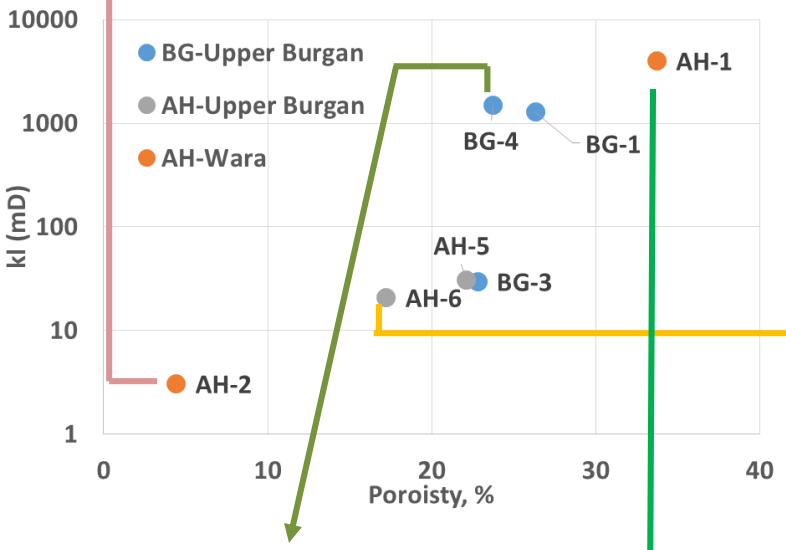

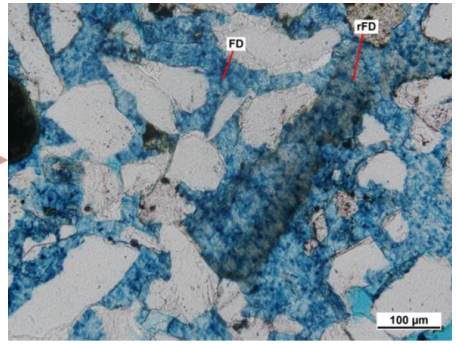

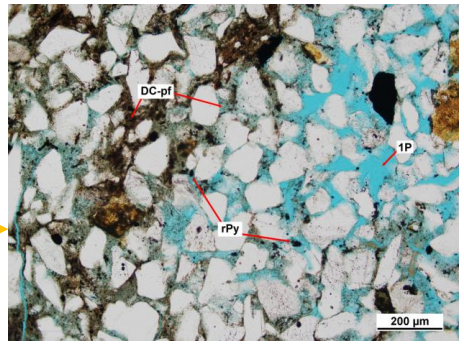

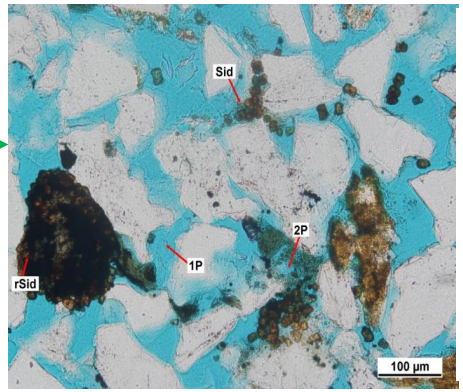

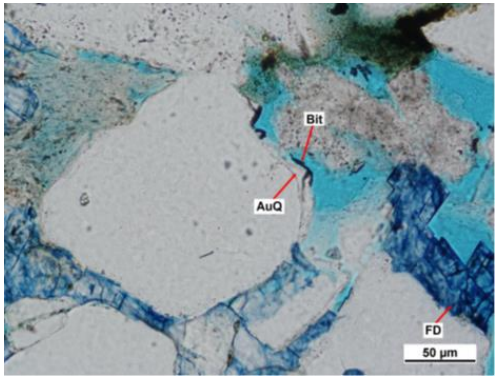

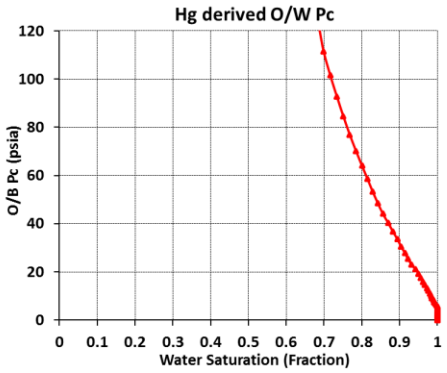

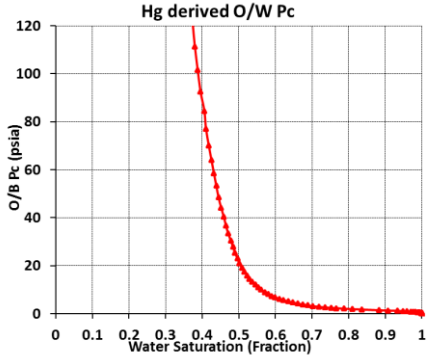

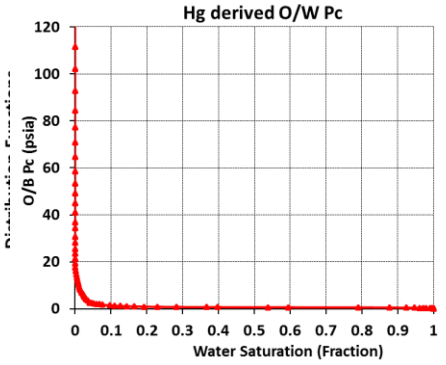

Enhancing the Reservoir Quality

Results and Data interpretation: Rock Typing

AAPG
Advancing the World of Petroleum Geosciences.

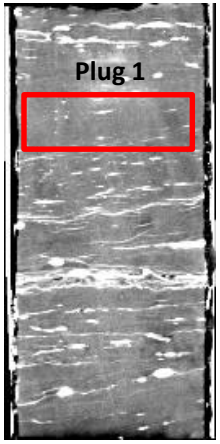

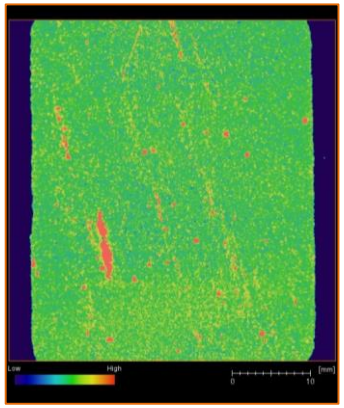

WF-RRT I

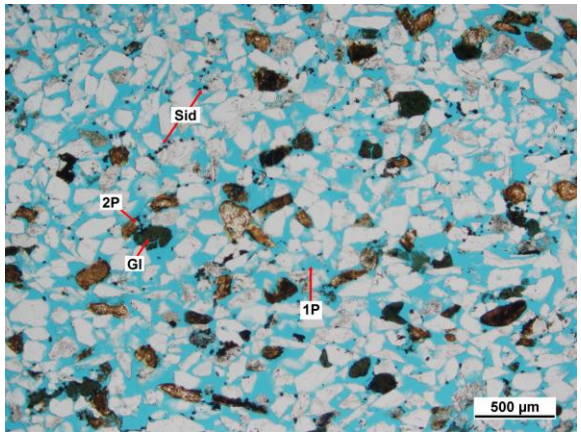

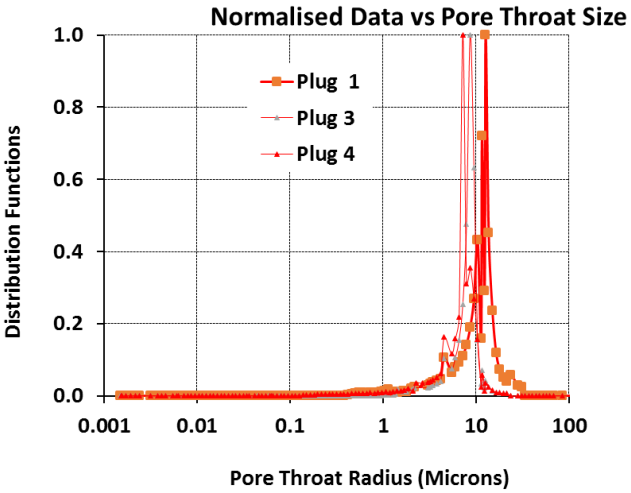

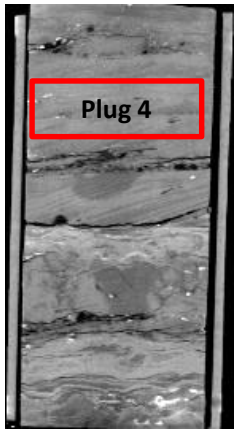

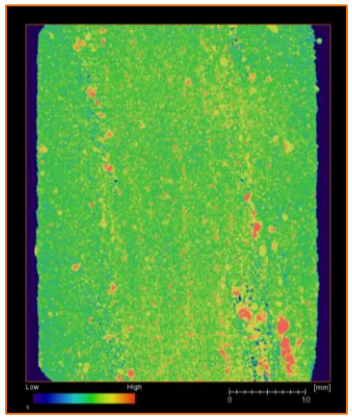

UBF- RRT I

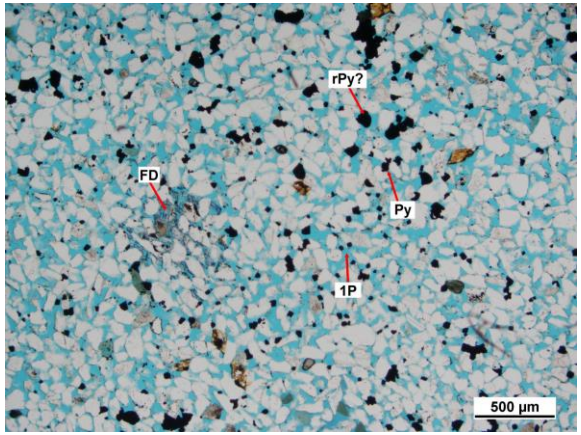

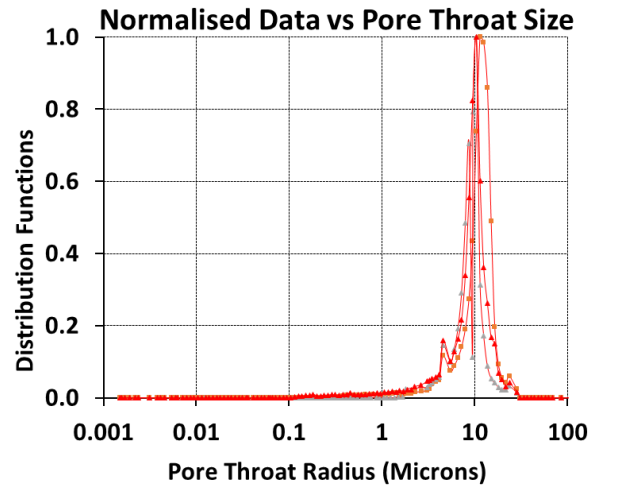

Results and Data interpretation: Rock Typing

AAPG
Advancing the World of Petroleum Geosciences.

WF-RRT II

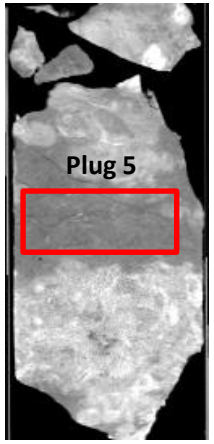

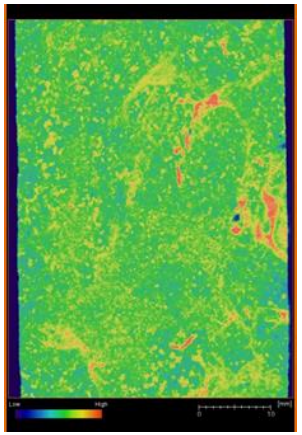

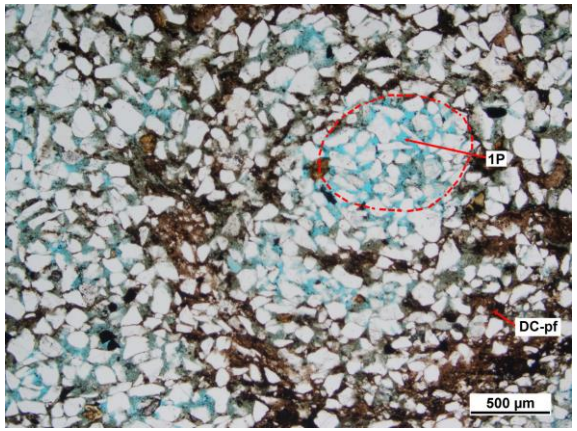

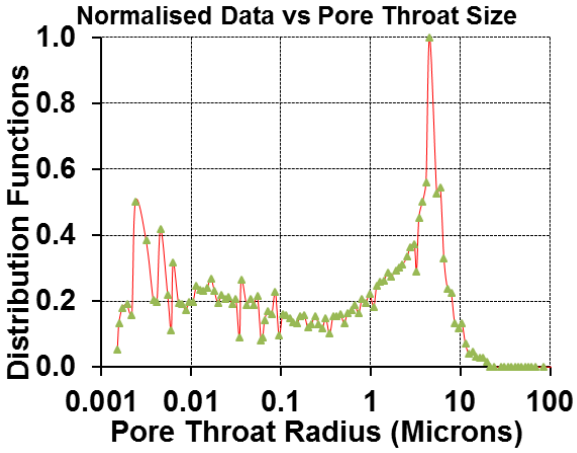

UBF- RRT II

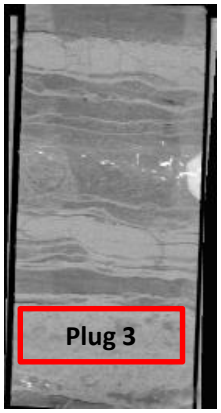

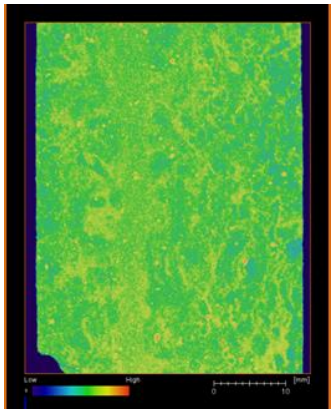

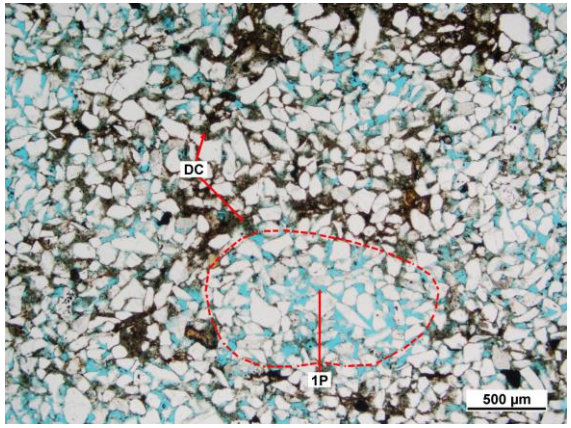

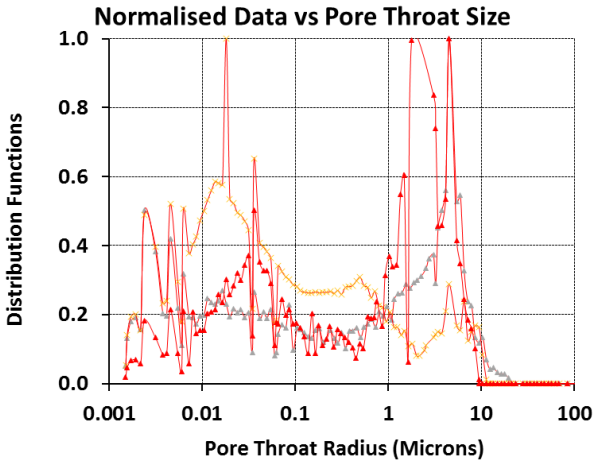

Results and Data interpretation: DRA (High Resolution Scanning)

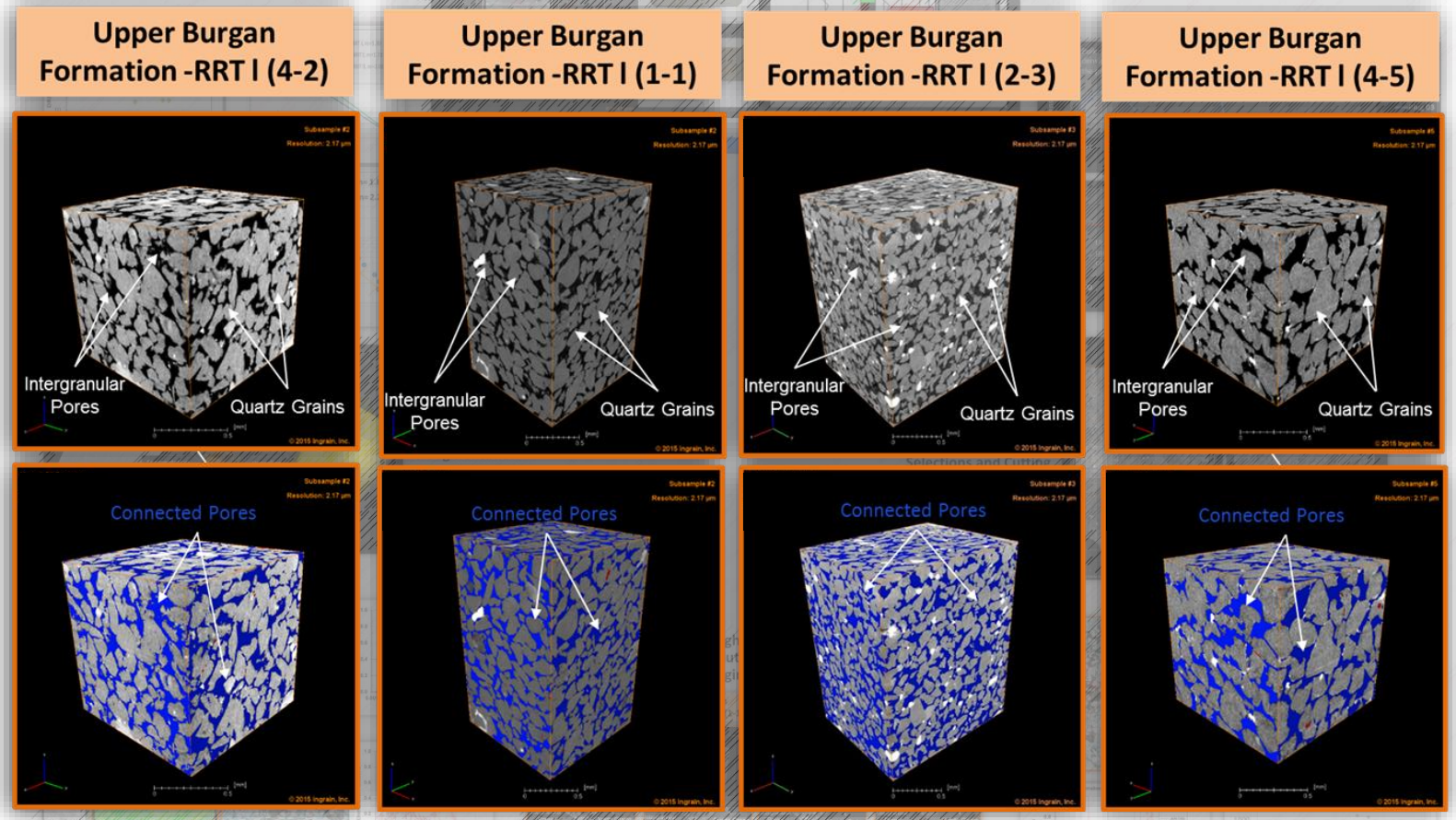

Results and Data interpretation: DRA (High Resolution Scanning)

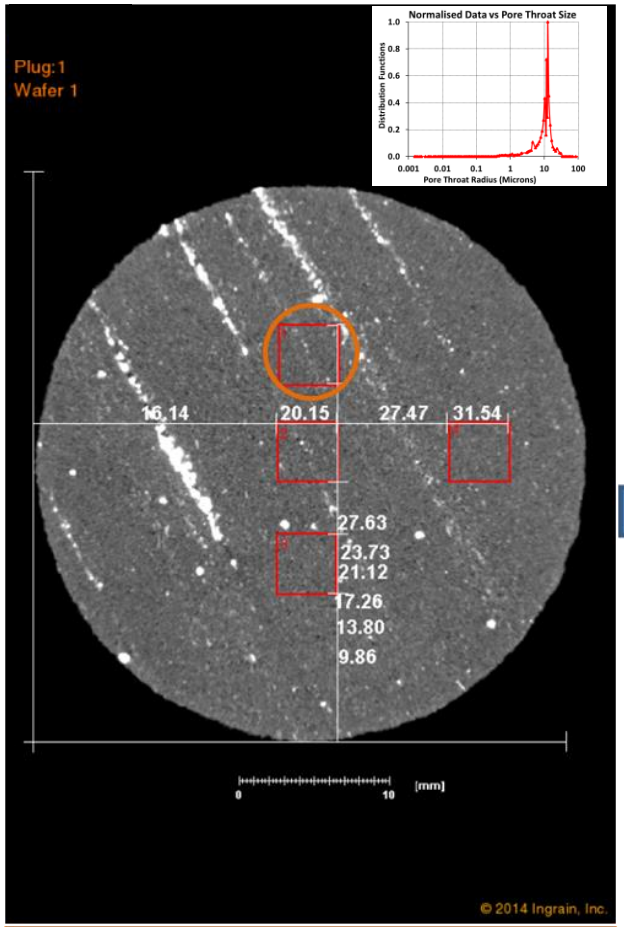

40 µm/voxel resolution scanning

3.77 µm/voxel resolution scanning

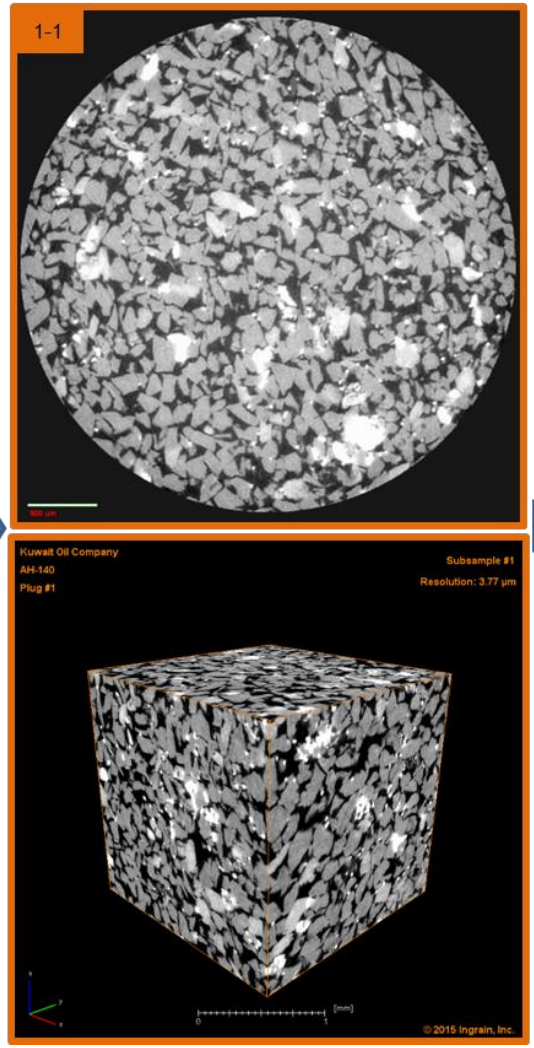

2.17 µm/voxel resolution scanning

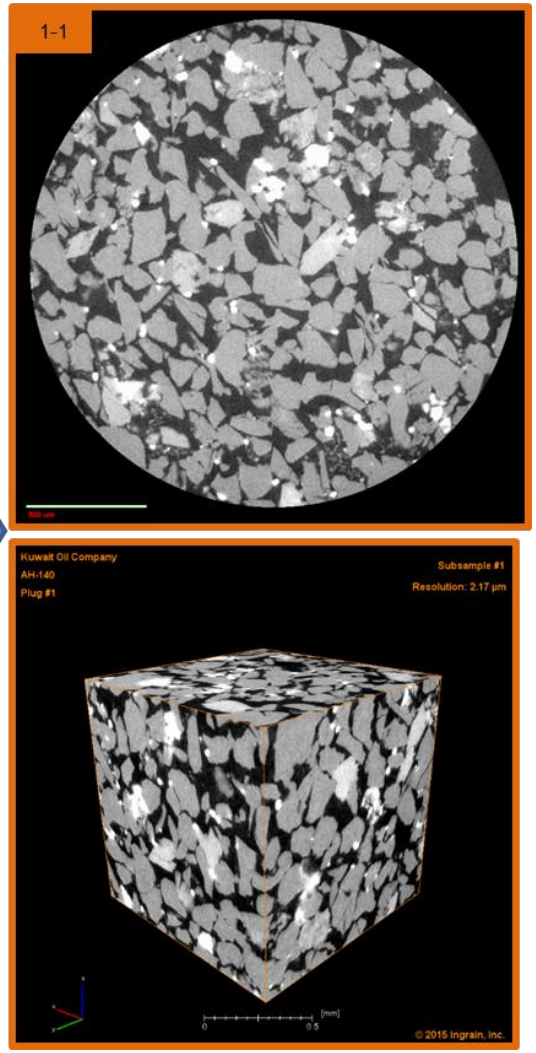

Based on MICP ; 2 µm/voxel resolution is needed to resolve the pore system of RRT I samples in both formations.

Results and Data interpretation: DRA (High Resolution Scanning)

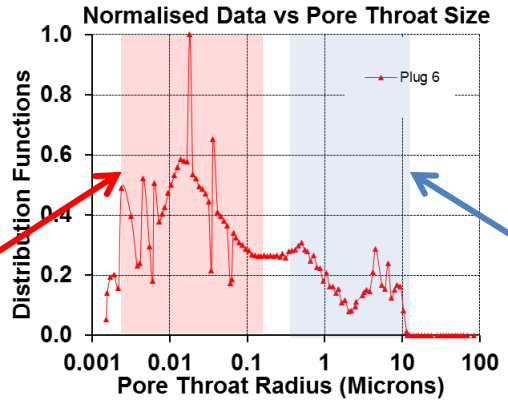

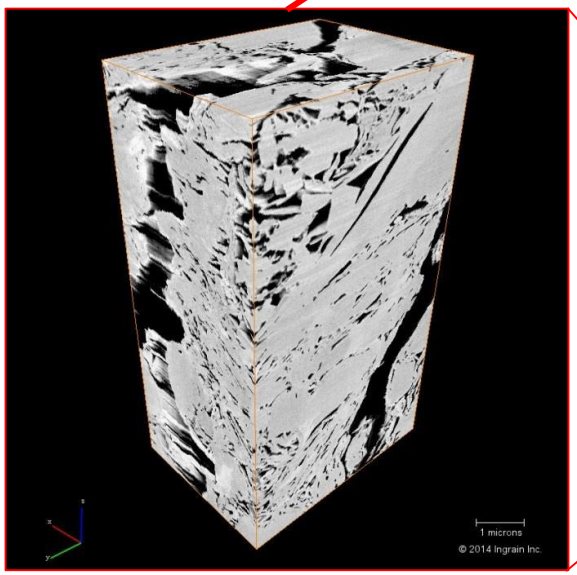

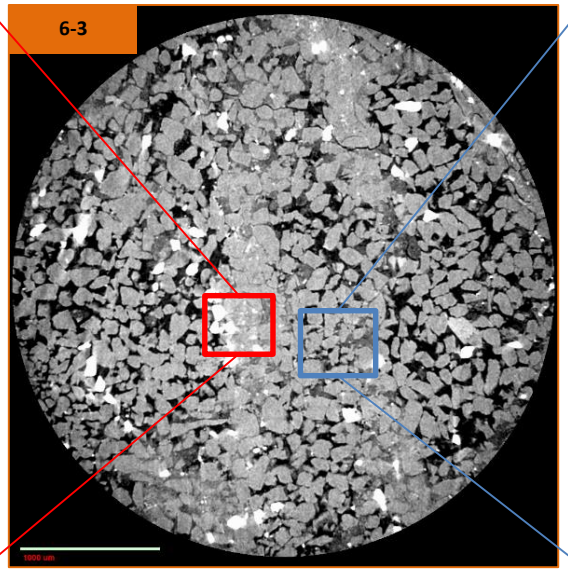

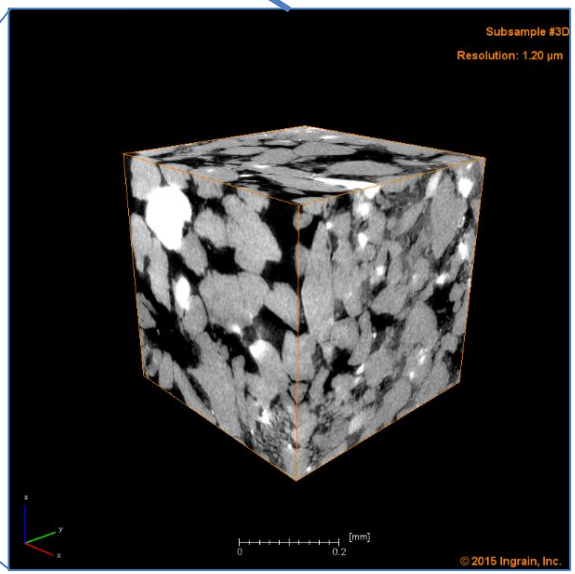

0.015 µm/voxel resolution scanning (FIB-SEM)

3.99 µm/voxel resolution scanning

1.20 µm/voxel resolution scanning

Based on MICP ; 1 and 0.015 µm/voxel resolutions were needed to resolve the pore system of RRT II samples in both formations.

AAPG
Advancing the World of Petroleum Geosciences.

Results and Data interpretation: DRA (Images Segmentation)

Wara and Upper Burgan RRTI

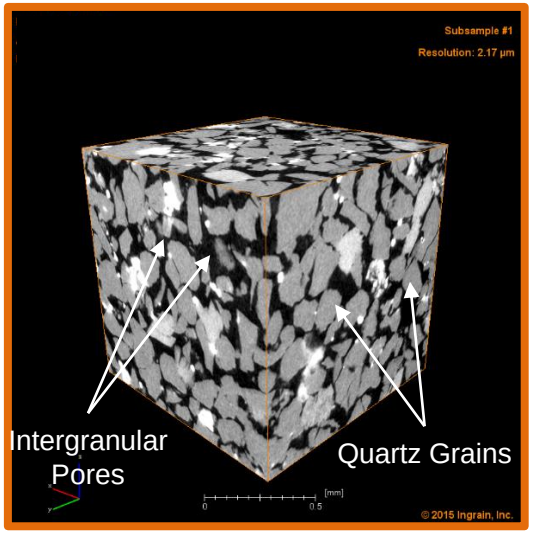

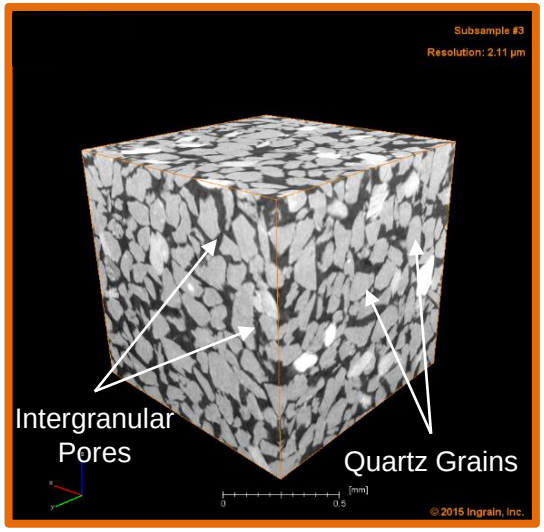

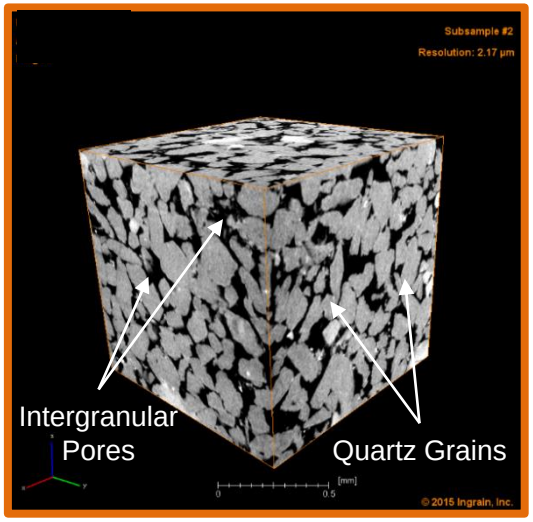

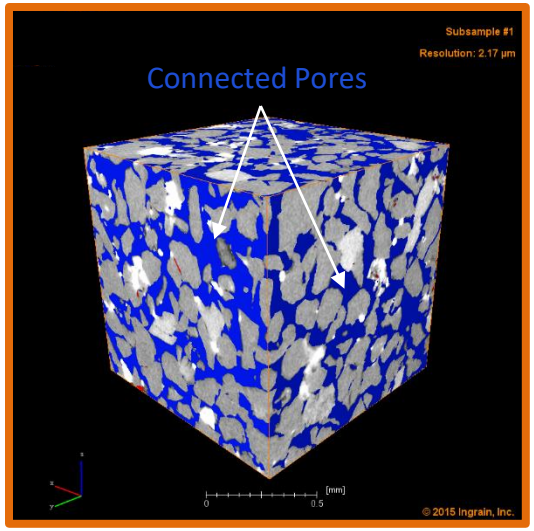

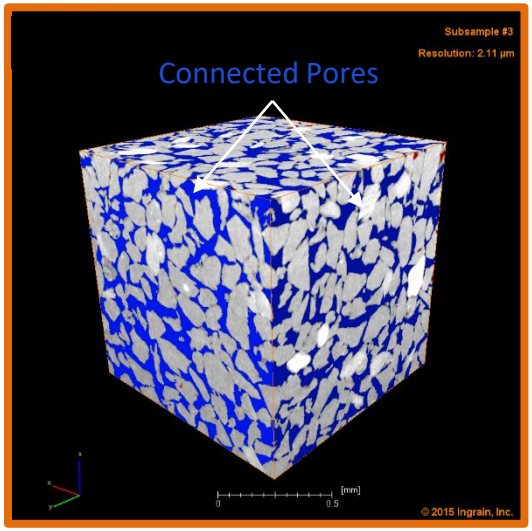

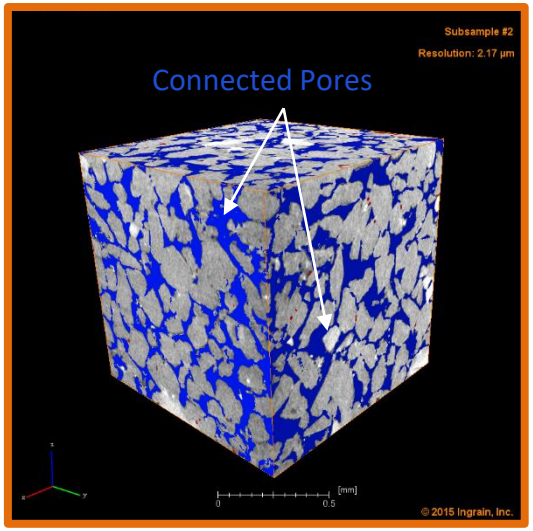

AAPG
Advancing the World of Petroleum Geosciences.

Results and Data interpretation: DRA (Images Segmentation)

Upper Burgan RRTII

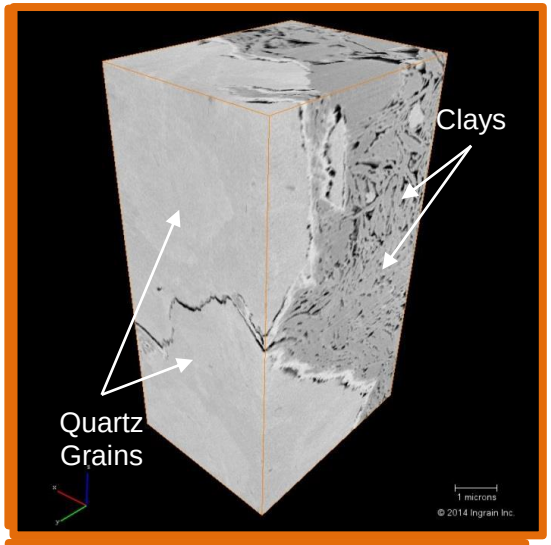

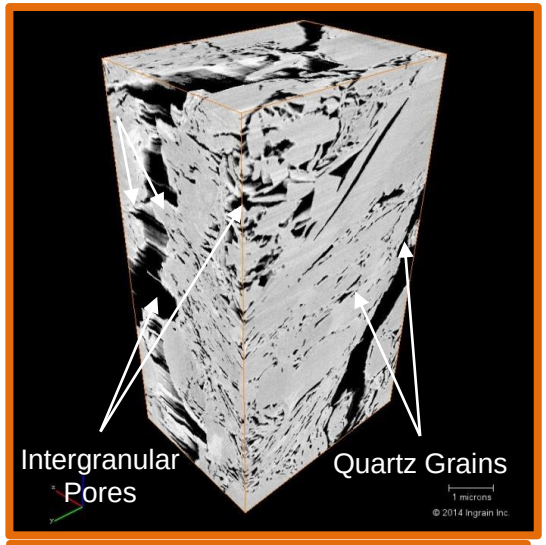

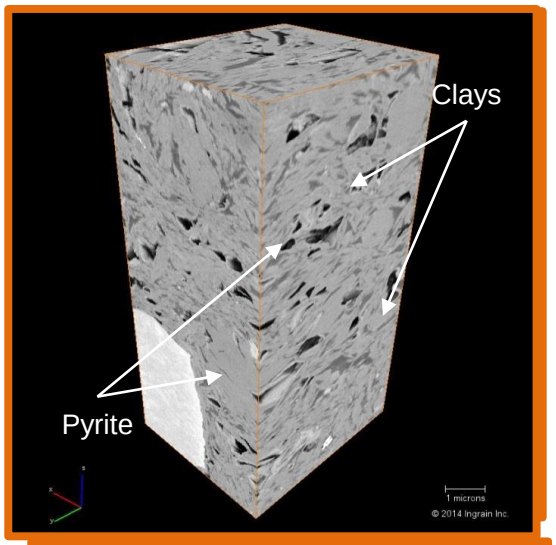

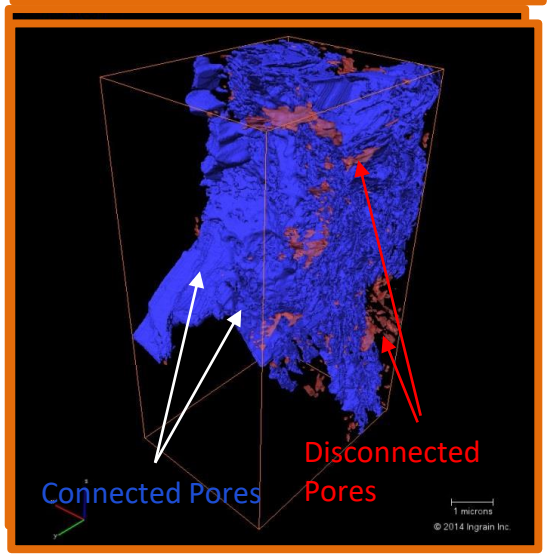

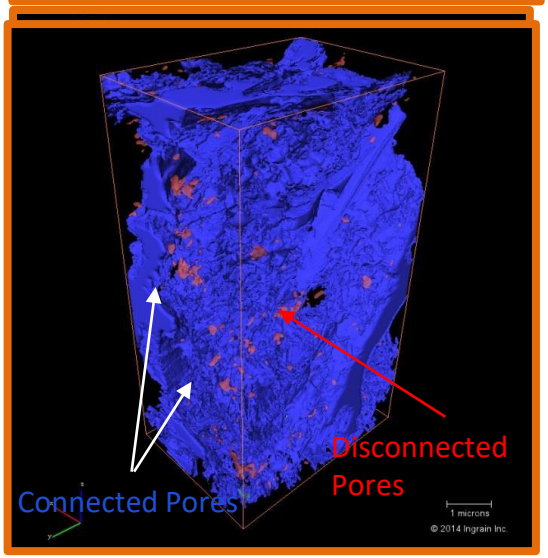

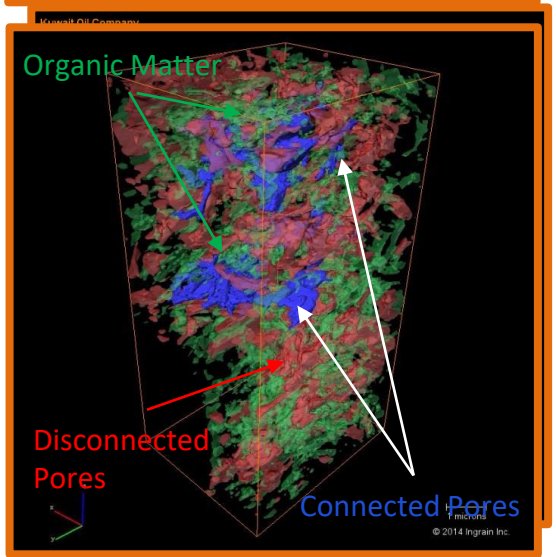

AAPG
Advancing the World of Petroleum Geosciences.

Results and Data interpretation: DRA (Numerical Computation)

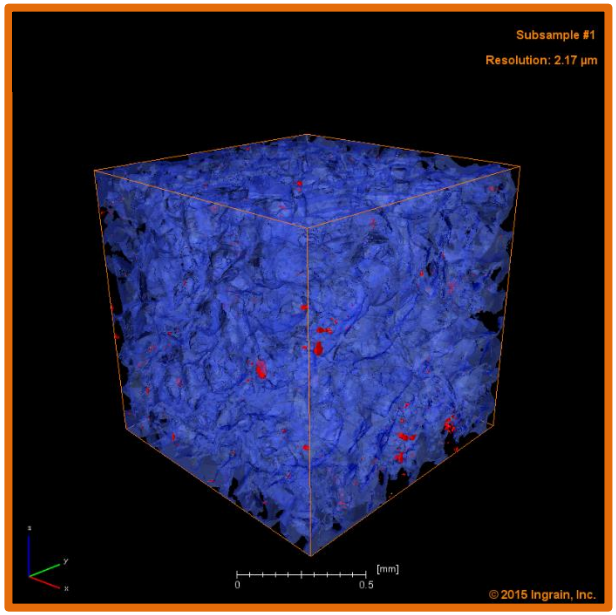

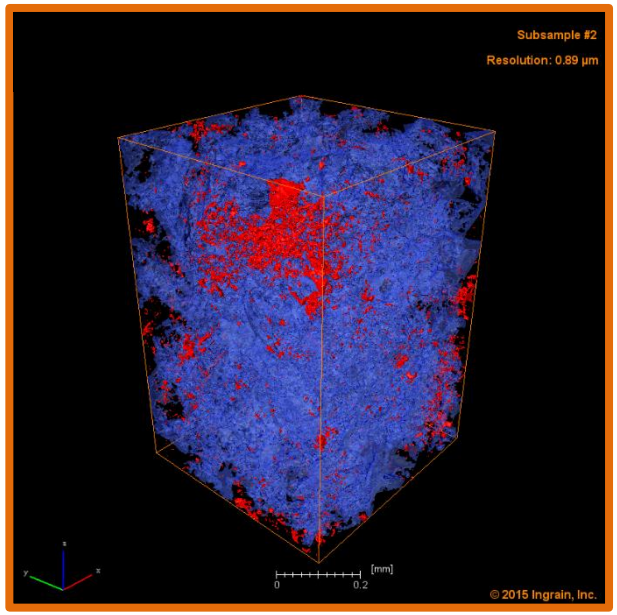

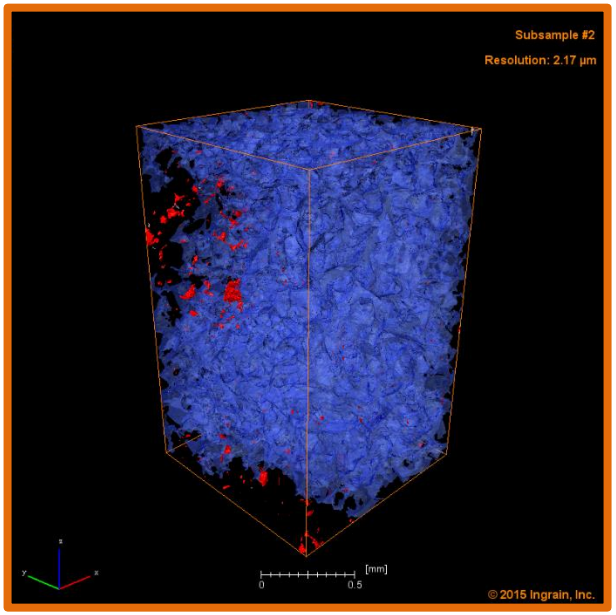

Numerical Computation at Subsamples Scale

Porosity	Absolute Permeability	PcRI	Relative Permeability	FRF
Segmentation	Lattice Boltzmann Method			Finite Element Method

Results and Data interpretation: DRA (Computation and Upscaling)

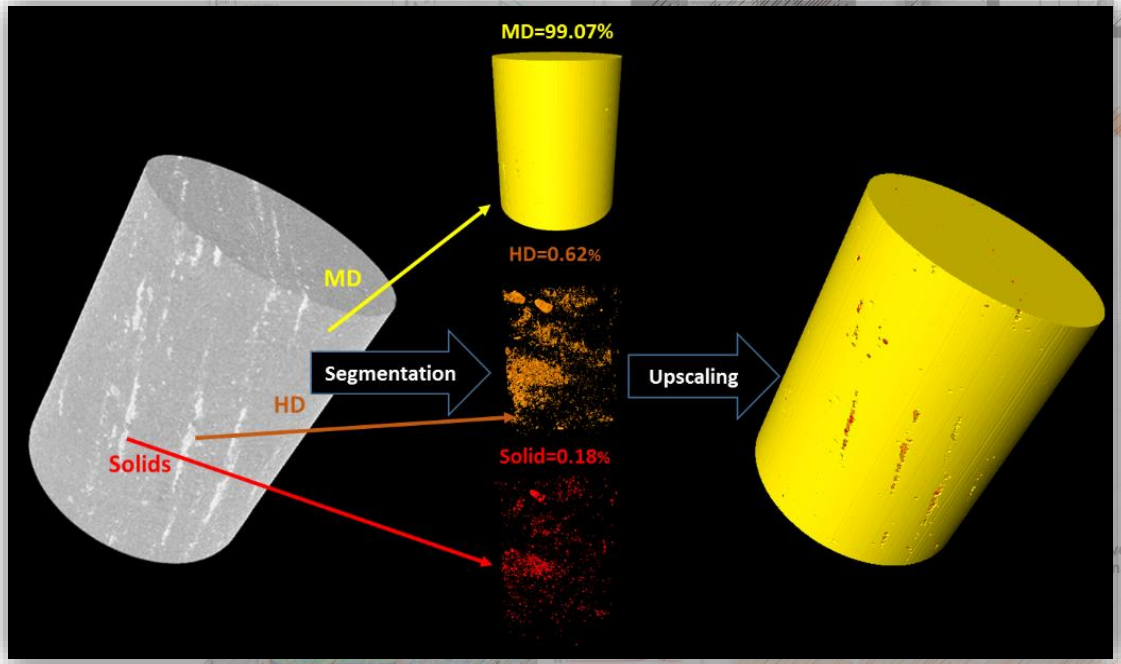

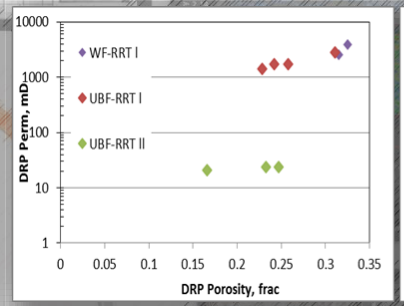

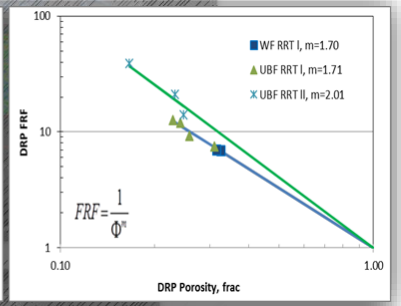

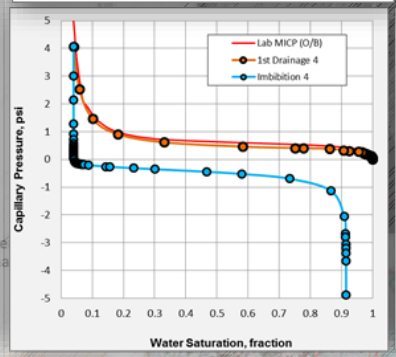

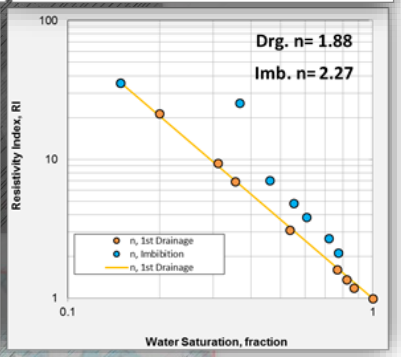

Results and Data interpretation: DRA (Computation and Upscaling)

- Before any advanced computation attempt; simulation of pore throat size distribution is done and results are compared with the physical lab MICP data.
- This is to insure that the pore system has been completely and properly captured and acquired 3D digital samples are real representation of the actual rock.

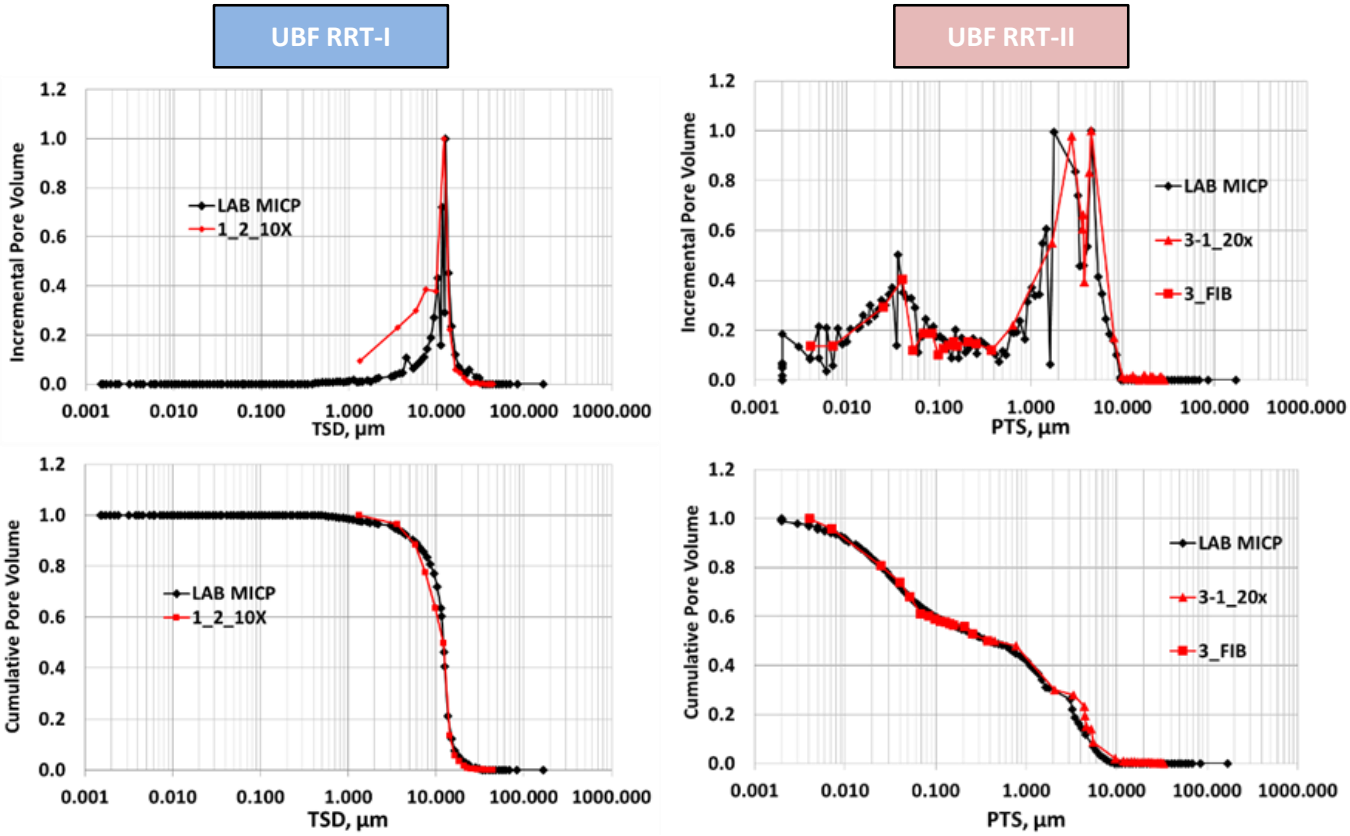

The simulated PTSD from these two sample form the same rock category showed excellent match with the lab MICP data.

Results and Data interpretation: : DRA (Upscaling to Plug Level)

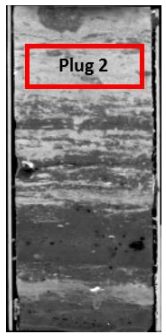

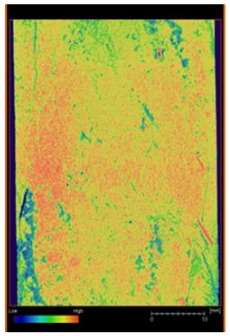

WF RRT-II

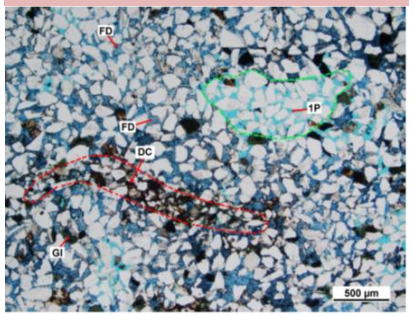

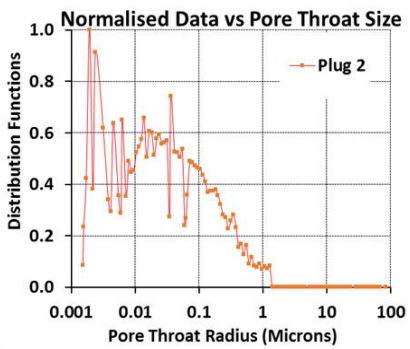

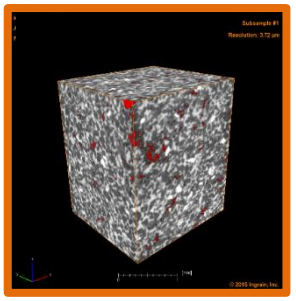

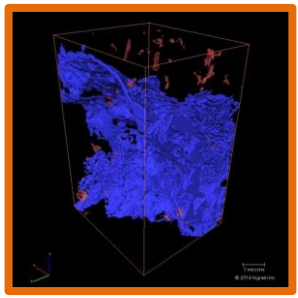

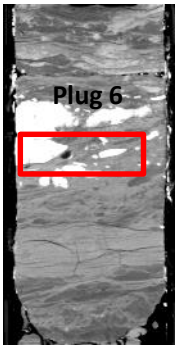

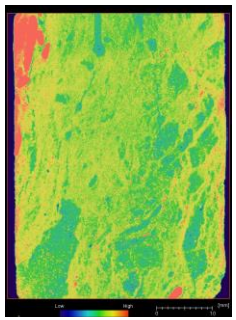

UBF- RRT II

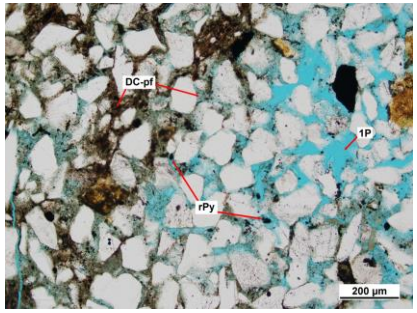

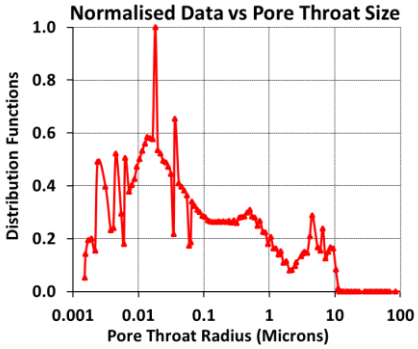

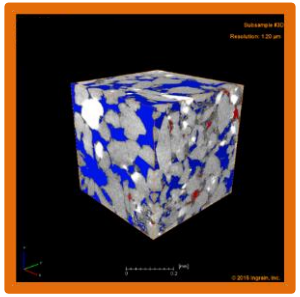

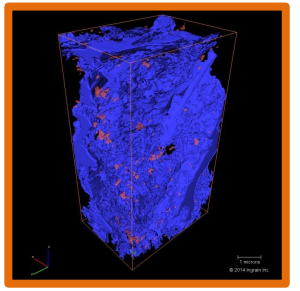

UBF- RRT II

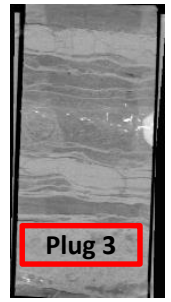

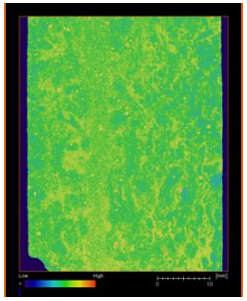

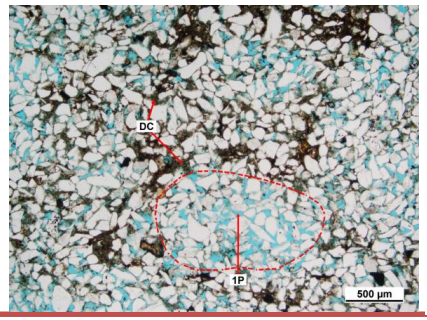

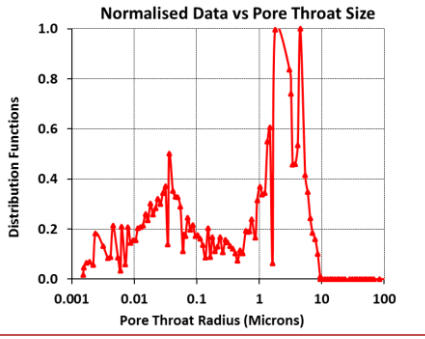

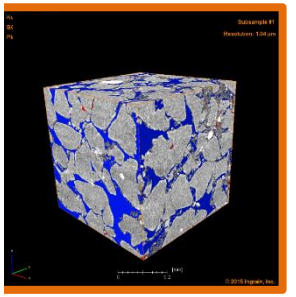

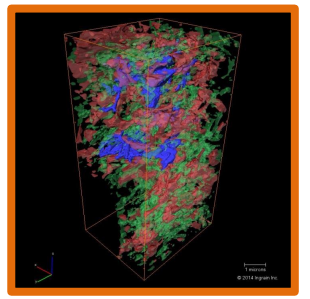

These samples were deemed unrepresentative and thus excluded from DRA computations.

AAPG
Advancing the World of Petroleum Geosciences.

Results and Data interpretation: DRA (Plug Segmentation)

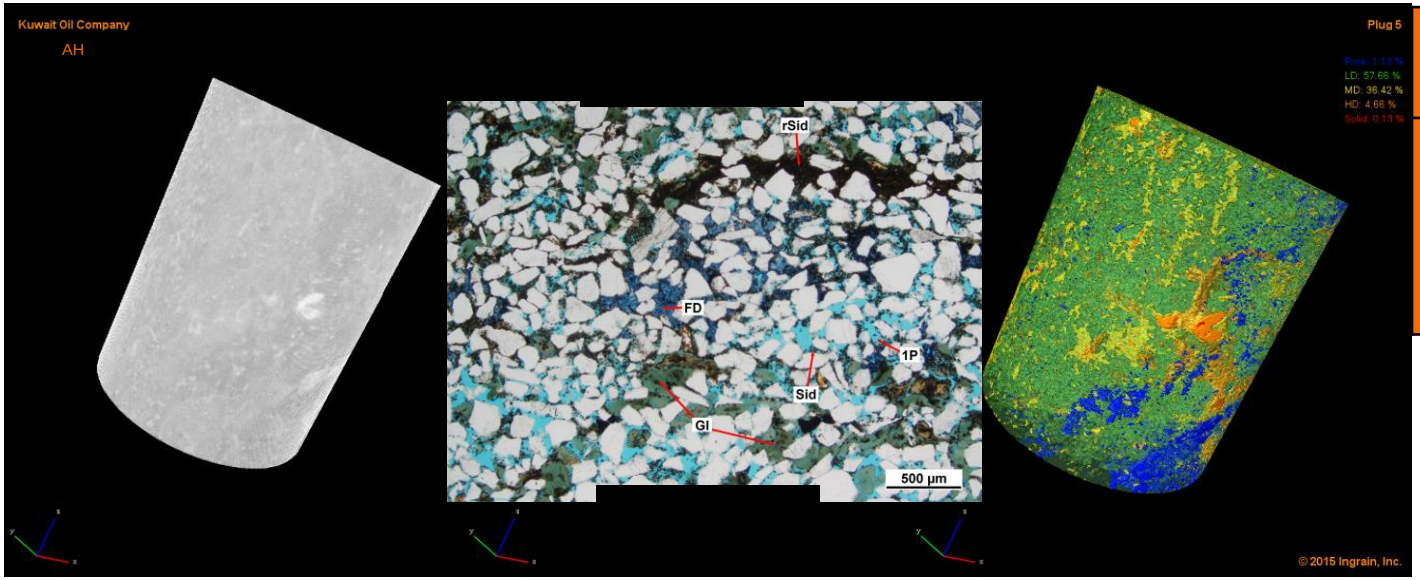

Rock Type	Phases	Phases Percentage (%)
UBF RRT II	Pore	1.13
	Low Dense	57.66
	Medium Dense	36.42
	High Dense	4.66
	Solid	0.13

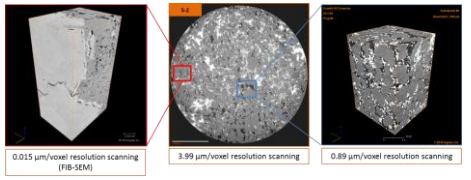

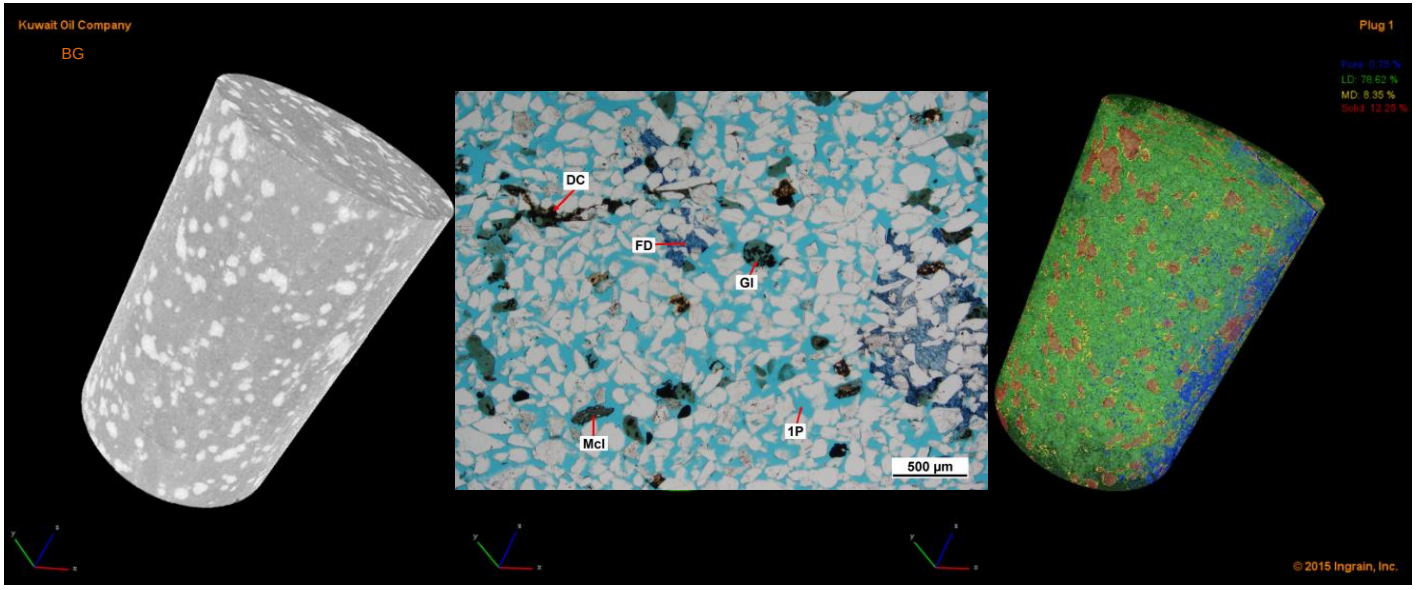

Rock Type	Phases	Phases Percentage (%)
UBF RRT I	Pore	0.78
	Low Dense	78.62
	Medium Dense	8.35
	Solid	12.25

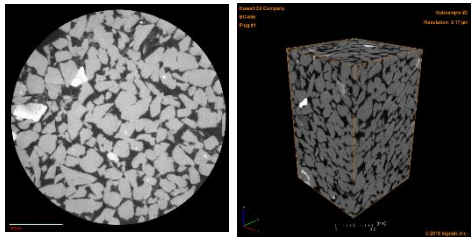

Results and Data interpretation: DRA (Upscaling Computed Data)

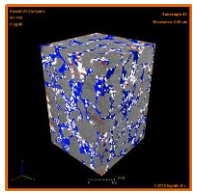

Porosity, Permeability, FRF, PcRI and Kr at Subsample Scale

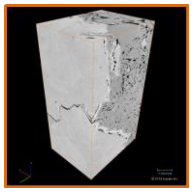

Upscaling the Computed Properties at Subsample Scale up to the corresponding Flow Unit with plug

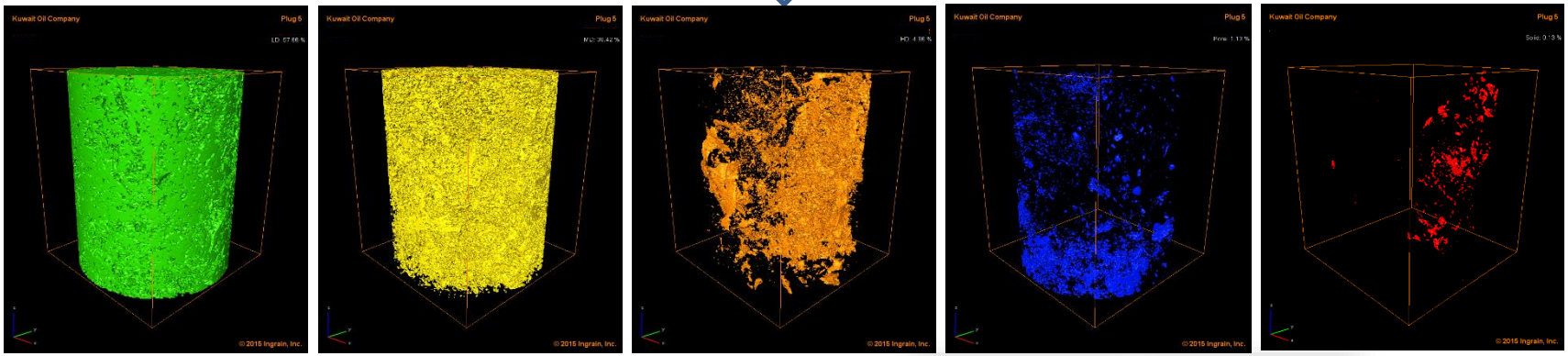

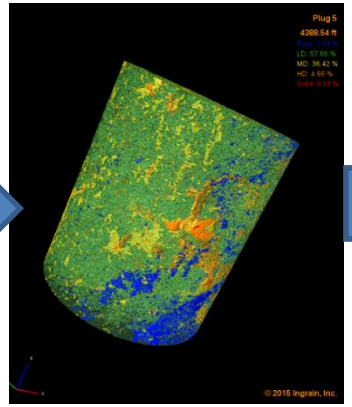

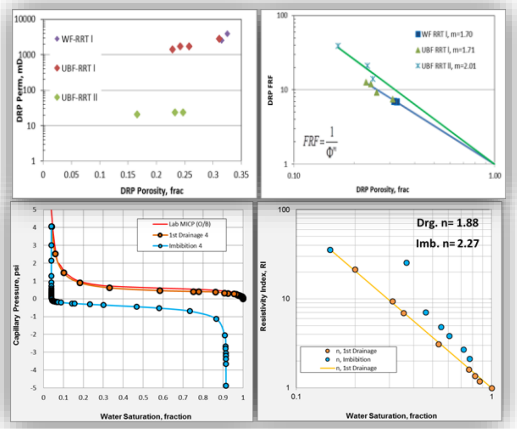

Results and Data interpretation: DRA (Upscaled RCA Properties)

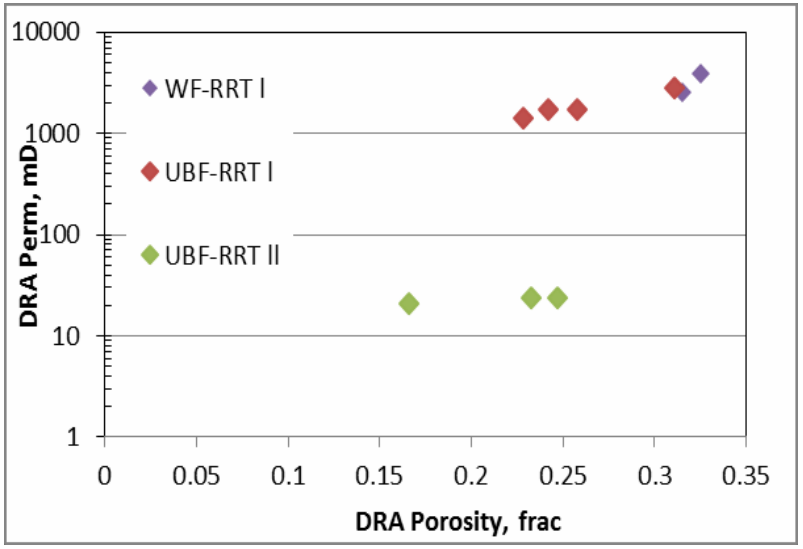

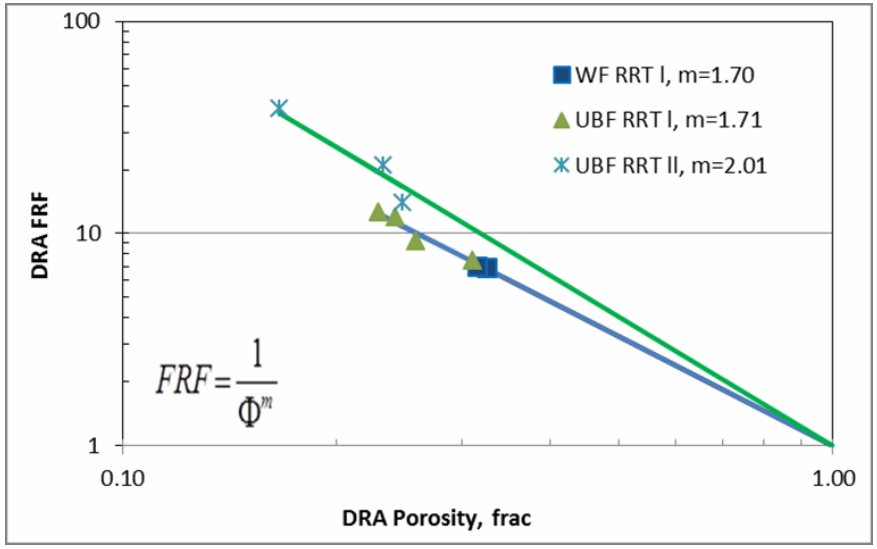

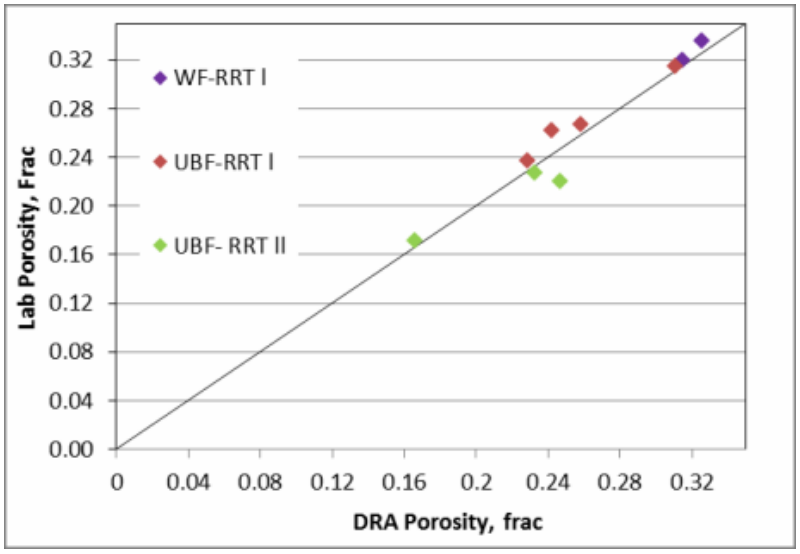

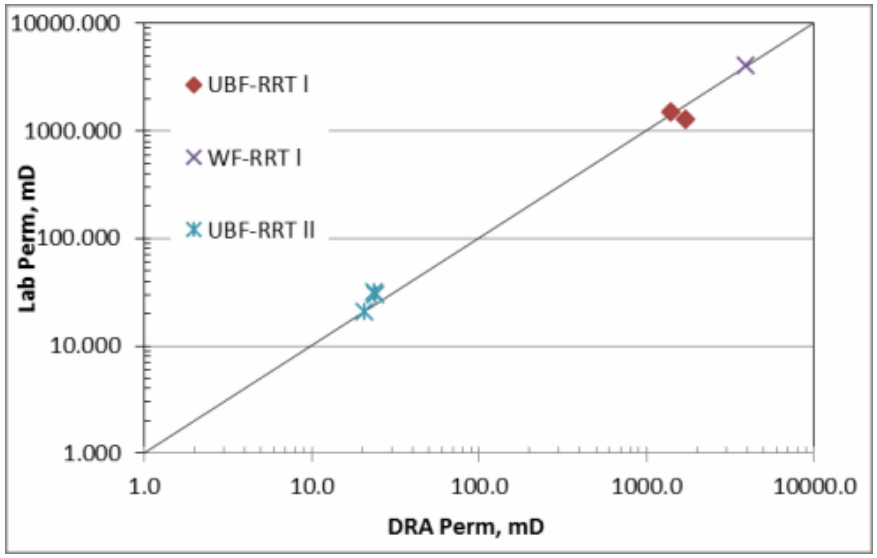

Results and Data interpretation: DRA (SCA: Upscaled PcRI)

Advancing the World of Petroleum Geosciences.

Fluid Properties were used by the simulator to compute SCA properties at subsample level.

Field	Brine (141°F and 1952 psi)		Oil (141°F and 1952 psi)		IFT	Contact Angle	
	Density (gm/cc)	Viscosity cp	Density (gm/cc)	Viscosity (cp)	(N/M)	Drainage	Imbibition
AH	NA	NA	0.771	1.433	0.03	30	130
BG	NA	0.64	NA	1.13	0.025	30	130

n =	2.45	n =	2.50
n, 1st Drainage		n, Imbibition	
Sw	RI	Sw	RI
1.0000	1.0000	0.2127	39.2218
0.8916	1.1311	0.7132	4.3905
0.8491	1.3488	0.7974	2.7030
0.7463	2.8601	1.0000	1.0000
0.4160	11.3262		
0.27	22.72		
0.21	39.22		

Upscaling to Plug Level

UBF-RRT I

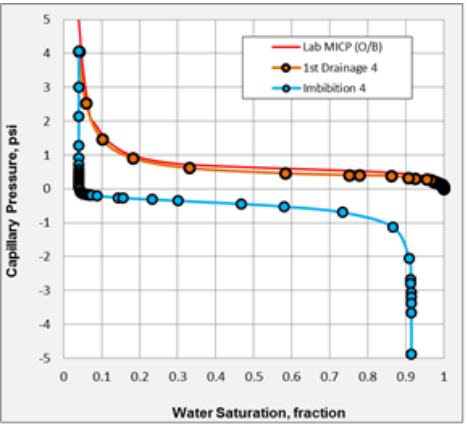

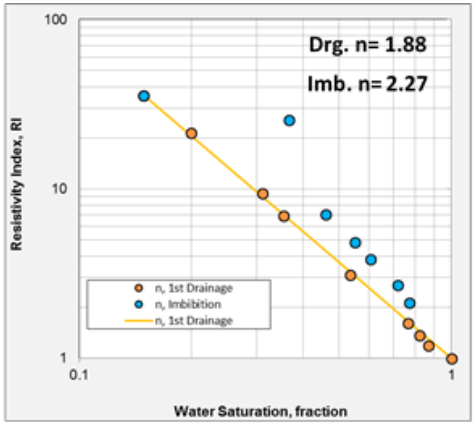

UBF-RRT II

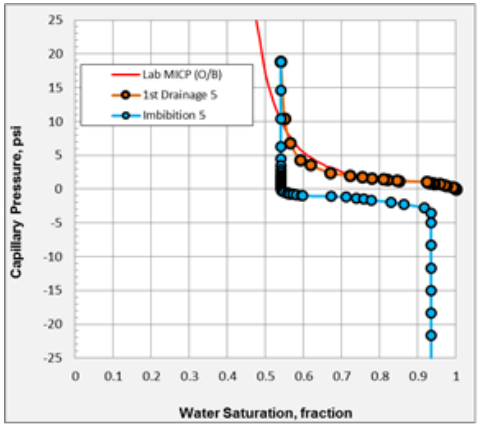

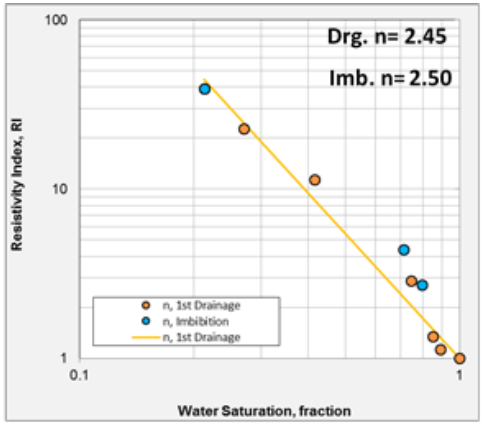

The computed PD in all samples matched very well with the corresponding MICP drainage data.

AAPG
Advancing the World of Petroleum Geosciences.

Results and Data interpretation: DRA (SCA: Upscaled Relative Permeability)

Fluid Properties were used by the simulator to compute SCA properties at subsample level.

Field	Brine (141°F and 1952 psi)		Oil (141°F and 1952 psi)		IFT	Contact Angle	
	Density (gm/cc)	Viscosity cp	Density (gm/cc)	Viscosity (cp)	(N/M)	Drainage	Imbibition
AH	NA	NA	0.771	1.433	0.03	30	130
BG	NA	0.64	NA	1.13	0.025	30	130

Upscaling to Plug Level

UBF-RRT I

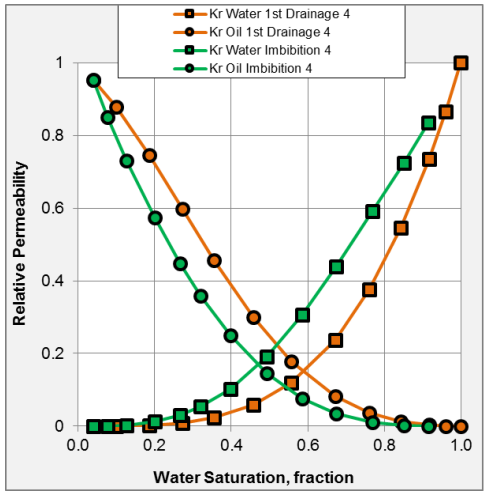

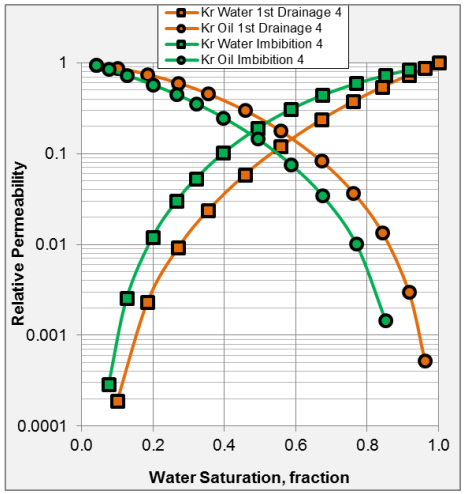

UBF-RRT II

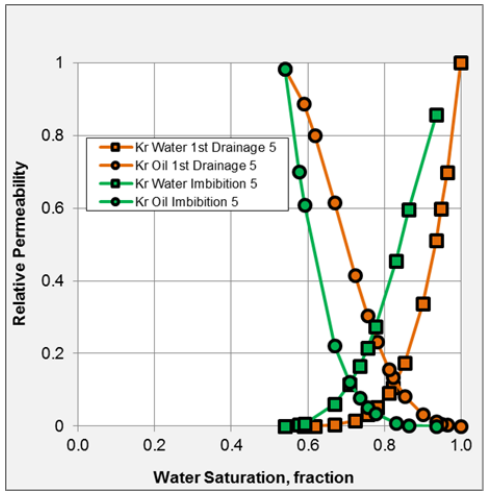

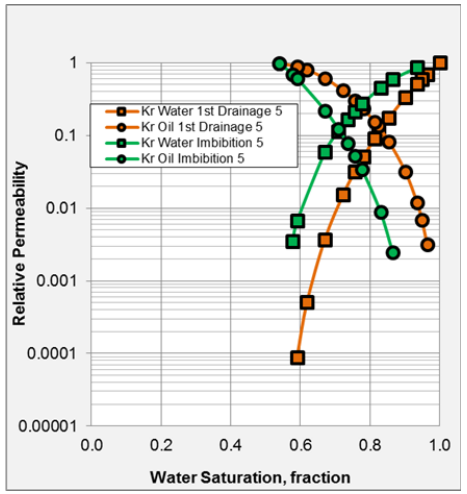

Kr end point saturations came inline with corresponding saturations from Pc which indicates data consistency

Summary and Conclusion

- In this study, total of 15 ft whole cores from Greater Burgan Field (The world largest siliciclastic Reservoir).
- The cores represents the Mid-Cretaceous siliciclastic successions of Wara and Upper Burgan Formation that deposited in a fluvial deltaic environment on the continental shelf margin of the ancient Tethys Ocean.
- These core were characterized using an integrative workflow taking in considerations the conventional and digital core analysis methods.

AAPG
Advancing the World of Petroleum Geosciences.

Summary and Conclusion

- The convectional core analysis methods including petrography, XRD, MICP and proper as well as the digital methods including high resolution and DE scanning affirms on two main rock types:
  - RRT I which characterized by very high porosity and permeability with narrow PTSD at 10 µm. It composed mainly of framework monocrystalline quartz grains in addition to common detrital K-Feldspar, plagioclase, opaque grains and traces of heavy minerals and clays. Clean primary inter-granular pore with very good connectivity are dominant.
  - RRT II which characterized by low porosity and permeability with bimodal PTSD 4.5 and 0.018 microns, respectively. It composed mainly made of both detrital clays and framework detrital monocrystalline quartz. The most dominate pore system in this rock type is the micro-pores hosted by clay minerals and \while the primary interparticle pores are rare and isolated.

Summary and Conclusion

- Up-scaled poroperm cross plots show a perfect linear relation.
- Upscaled primary drainage and imbibition Kr's showed similar end points to the corresponding Pc cycles.
- Residual oil saturation (S_{or}) defined by the imbibition Pc curves of WF and UBF is in the range of approximately 6%.
- Pores within clay minerals in sample AH-5 remained water filled and this explains the high Swi in this sample.
- The Up-scaled Krw curves and end points in WF/ UBF RRT l indicate oil wet behavior (Krw end points in the range of 0.836 to 0.901); this is in line with the observed forced imbibition from Pc computations.

AAPG

Advancing the World of Petroleum Geosciences.

Acknowledgment

The authors would like to thank KOC for their contributions and support through the course of this study. The keen interest shown by Laila Hayat and Mona Rashied is gratefully acknowledged.

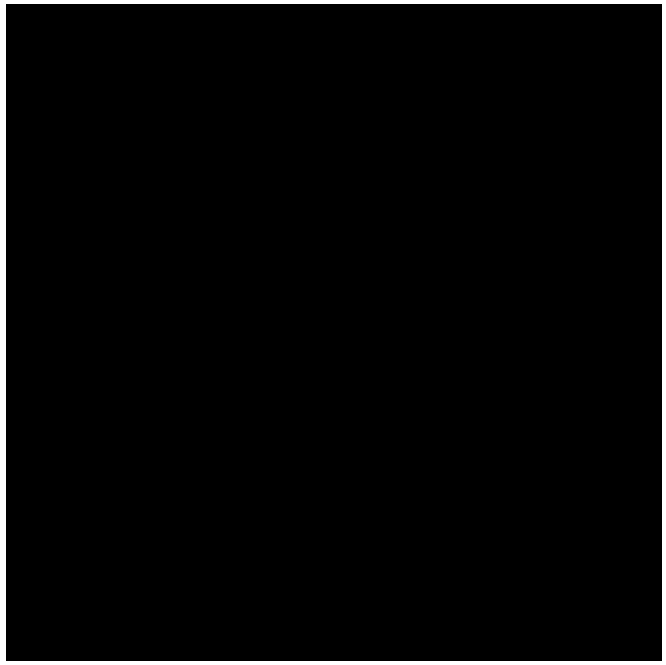

Kuwait Oil Company

A Subsidiary of Kuwait Petroleum Corporation

INGRAIN